frontiers | Frontiers in Immunology

TYPE Original Research
PUBLISHED 04 December 2025
DOI 10.3389/fimmu.2025.1692382

OPEN ACCESS

EDITED BY
Oscar J. Cordero,
University of Santiago de Compostela, Spain

REVIEWED BY
Jonadab Efrain Olguin Hernandez,
National Autonomous University of Mexico, Mexico
Jian Li,
Mianyang Third People's Hospital, China

*CORRESPONDENCE
Mayte Coiras
mcoiras@isciii.es
José Perea
josepereag@hotmail.com

†These authors have contributed equally to this work

RECEIVED 25 August 2025
REVISED 04 November 2025
ACCEPTED 10 November 2025
PUBLISHED 04 December 2025

CITATION
Sánchez-Menéndez C, Rodríguez-Pérez J, Fuertes D, Leguizamon V, González-Sanmartín M, Mateos E, Cervero M, San José E, Sanz G, Álvaro E, Ballestero-Pérez A, Martí-Gallostra M, Rueda JA, Hurtado-Caballero E, Pastor C, Balaguer F, Spinelli A, Martínez-Laso J, Torres M, Perea J and Coiras M (2025) Differences in the peripheral blood immune landscape between early-onset and late-onset colorectal cancer. *Front. Immunol.* 16:1692382. doi: 10.3389/fimmu.2025.1692382

Differences in the peripheral blood immune landscape between early-onset and late-onset colorectal cancer

Clara Sánchez-Menéndez[1,2], Jaime Rodríguez-Pérez[1,3], Daniel Fuertes[4], Valentina Leguizamon[1,2,5], María González-Sanmartín[1,6], Elena Mateos[1,7], Miguel Cervero[8], Esther San José[9], Gonzalo Sanz[10], Edurne Álvaro[11], Araceli Ballestero-Pérez[12], Marc Martí-Gallostra[13], José Antonio Rueda[14], Elena Hurtado-Caballero[15], Carlos Pastor[16], Francesc Balaguer[17,18,19,20], Antonino Spinelli[21,22], Jorge Martínez-Laso[23], Montserrat Torres[1,7†], José Perea[24,25*] and Mayte Coiras[1,7*†] on behalf of the Spanish EOCRC Consortium (SECOC)

[1]Department of Hematology and Hemotherapy, Instituto Ramón y Cajal de Investigación Sanitaria (IRYCIS), Hospital Universitario Ramón y Cajal, Majadahonda, Madrid, Spain, [2]PhD Program in Biomedical Sciences and Public Health, Universidad Nacional de Educación a Distancia (UNED), Madrid, Spain, [3]Faculty of Biological Sciences, Universidad Complutense de Madrid, Madrid, Spain, [4]School of Telecommunications Engineering, Universidad Politécnica de Madrid, Madrid, Spain, [5]Department of Hematology and Hemotherapy, Instituto Ramón y Cajal de Investigación Sanitaria (IRYCIS), Hospital Universitario Ramón y Cajal, Madrid, Spain, [6]Faculty of Biological Sciences, Universidad de Alcalá, Madrid, Spain, [7]Biomedical Research Center Network in Infectious Diseases (CIBERINFEC), Instituto de Salud Carlos III, Majadahonda, Madrid, Spain, [8]Facultad de Ciencias Biomédicas y de la Salud, Universidad Alfonso X el Sabio (UAX), Madrid, Spain, [9]Department of Medicine, Faculty of Medicine, Health and Sports, Universidad Europea de Madrid, Madrid, Spain, [10]Surgery Department, San Carlos University Hospital, Madrid, Spain, [11]Surgery Department, Infanta Leonor University Hospital, Madrid, Spain, [12]Surgery Department, Ramon y Cajal University Hospital, Madrid, Spain, [13]Colorectal Unit, Vall d´Hebrón University Hospital, Universitat Autónoma de Barcelona (UAB), Barcelona, Spain, [14]Surgery Department, Alcorcon Foundation Hospital, Madrid, Spain, [15]Surgery Department, Gregorio Marañon University Hospital, Madrid, Spain, [16]Navarra University Clinic (Clínica Universidad de Navarra), Pamplona, Navarra, Spain, [17]Department of Gastroenterology, Hospital Clínic de Barcelona, Barcelona, Spain, [18]Institut d'Investigacions Biomèdiques August Pi i Sunyer (IDIBAPS), Barcelona, Spain, [19]Centro de Investigación Biomédica en Red de Enfermedades Hepáticas y Digestivas (CIBEREHD), Barcelona, Spain, [20]University of Barcelona, Barcelona, Spain, [21]Department of Biomedical Sciences, Humanitas University, Milan, Italy, [22]Istituto di Ricovero e Cura a Carattere Scientifico (IRCCS) Humanitas Research Hospital, Milan, Italy, [23]Immunogenetics Unit, National Center of Microbiology, Instituto de Salud Carlos III, Majadahonda, Madrid, Spain, [24]Biomedical Research Institute of Salamanca (IBSAL), Salamanca, Spain, [25]Coloproctology Unit, Hospital Universitario Vithas Madrid Arturo Soria, Madrid, Spain

Introduction: Colorectal cancer (CRC) is a leading cause of cancer-related mortality. While screening has reduced incidence in older adults, cases of early-onset CRC (EOCRC), diagnosed before age 50, are rising, highlighting the need to understand its unique biology. Immune responses, particularly T-cell infiltration measured by the tumor-based Immunoscore, are known predictors of CRC prognosis, but less is known about systemic immune differences by age at diagnosis.
Methods: Peripheral blood mononuclear cells (PBMCs) from EOCRC (n=19) and late-onset CRC (LOCRC; n=19) participants recruited in Madrid (Spain) were analyzed for immune cell phenotypes, exhaustion markers, soluble cytokines, and metabolic activity.

Results: Our study revealed distinct peripheral blood immune profiles differentiating EOCRC from LOCRC. EOCRC patients exhibited a heightened proinflammatory environment, with increased functional capacity of CD4+ Th1, Th9, and Th17 subsets to produce IFNg, IL-9, and IL-17A, respectively, and increased plasma levels of IFNg and CXCL8/IL-8. This suggests an active but potentially ineffective immune response. Conversely, LOCRC patients showed hallmarks of immunosenescence and chronic inflammation, including impaired cytokine production, higher frequencies of CD8+ Tgd and Th22 cells, and increased plasma CCL13/MCP-4, consistent with tissue remodeling and immune suppression. Biomarkers distinguishing EOCRC included reduced Th22 and CD8+ Tgd cell frequencies and higher NKT-like cells with increased IL-13 production by Th22 cells.

Conclusions: EOCRC and LOCRC involved different immune mechanisms, where EOCRC showed an altered proinflammatory environment with preserved regulatory pathways, while LOCRC reflected age-related immune decline and inflammaging. Peripheral blood immune profiling offers a minimally invasive liquid Immunoscore for early detection and enables personalized immunotherapies for age-related immune landscapes, particularly benefiting younger individuals at risk of EOCRC.

KEYWORDS

colorectal neoplasms, early diagnosis, immune response, T-cell subsets, cytokine profiling, immune biomarkers

1 Introduction

Colorectal cancer (CRC) is the second most common cancer among women and the third most common among men in the Western world. In 2022, it accounted for 9.6% of all new cancer cases worldwide and was the second leading cause of cancer-related mortality, responsible for 9.3% of deaths (1). Widespread screening for precancerous lesions has led to a decline in the incidence of CRC in most Western countries since the 1990s, particularly among adults aged 65 and older (2, 3). However, this positive trend masks an alarming increase in early-onset CRC (EOCRC), defined as cases diagnosed before age 50.

CRC incidence in adults aged 40 to 49 years has increased by almost 15% since 2000 (4), and in 2017, 10.5% of new CRC cases were reported in people younger than 50 years (5). While CRC incidence has declined in people aged 65 and older since 2011, rates have remained steady in those aged 50–64 and have increased by about 2% per year in individuals under 50 and the 50–54 age group (3). The rising incidence of EOCRC is remarkably higher in some countries, such as the US or Canada, and in other regions, as in Europe, heterogenous patterns of EOCRC incidence have been reported (6, 7).

Multiple studies have demonstrated that EOCRC tumors are clinically and pathologically distinct from late-onset CRC (LOCRC). EOCRC patients present with higher rates of microsatellite instability (MSI), mainly due to mismatch repair deficiency (7–9), differences in CpG island methylation phenotype (7), unique DNA methylation patterns linked to aging (10), and altered chromosomal regions (11), with distinct chromosomal instability and mutation profiles (8, 12, 13). Moreover, EOCRC is unlikely related to inflammaging, the chronic low-grade inflammation associated with aging that characterizes LOCRC (11, 14). These biological and molecular differences may contribute to the distinct clinical behavior and diagnostic challenges observed in EOCRC. The positive association between common CRC symptoms and a later diagnosis is much stronger in individuals under 50 than in those over 50 (8, 9). However, the time between symptoms first appearing and diagnosis is still months long, due to low awareness of symptoms by primary care providers, which significantly reduces their possibilities of survival (10, 15). Therefore, the search for more accurate early diagnostic and prognostic biomarkers for EOCRC is currently a priority.

Present preventive and therapeutic approaches are increasingly focused on the tumor microenvironment and the development of an efficient anticancer immunity (16–18). Due to an overall stronger immune response correlates to better outcomes in cancer patients, high density of cytotoxic cells, memory cells, and tumor infiltrating T cells (TILs) are considered biomarkers of survival (16, 19). Therefore, a consensus Immunoscore has been developed as a standardized, reproducible assay that may accurately predict recurrence risk and overall survival in CRC by primarily quantifying mostly CD3+ and CD8+ T-cell infiltration in the tumor center and invasive margin

(20). Patients with high Immunoscores showed lower risk of recurrence than those with low Immunoscores. Therefore, the marked differences between EOCRC and LOCRC have sparked interest in analyzing the role of the immune system in EOCRC development. However, because the Immunoscore relies on postoperative tumor specimens, its utility is restricted to prognosis after diagnosis rather than prevention or early detection, limitations particularly critical for EOCRC.

Despite the recognized importance of immune responses in CRC prognosis and the striking clinical differences between EOCRC and LOCRC, systemic immune profiles in peripheral blood have not been systematically compared between these age groups. Given that peripheral blood immune cells reflect systemic immune status and may provide accessible biomarkers, understanding how the circulating immune landscape differs between EOCRC and LOCRC could enable the development of minimally invasive diagnostic tools. A peripheral blood-based "liquid Immunoscore" could offer preventive and early-detection capabilities that the tissue-based Immunoscore cannot provide, potentially identifying high-risk individuals before tumors become clinically detectable.

This study aims to discover novel immune biomarkers specific to EOCRC that may permit the development of a non-invasive, peripheral blood-based "liquid Immunoscore" that may integrate specific quantitative measurements. By contrasting the immune landscapes of EOCRC and LOCRC based on key immune cell subsets, exhaustion markers, soluble cytokines, and metabolic capacity, we seek to improve early detection, enable more timely and personalized treatment, and ultimately identify individuals under 50 at high risk for EOCRC before tumors become clinically detectable.

2 Materials and methods

2.1 Participants

For this cohort study, participants diagnosed with EOCRC (n=19) were enrolled in Madrid (Spain) through the Spanish EOCRC Cohort (SECOC) (21). Patients with LOCRC (n=19) were also recruited for comparison. The inclusion criteria for EOCRC required participants to be over 18 years old but under 50 years old and have a confirmed diagnosis of CRC. Similarly, the inclusion criteria for LOCRC were to be over 50 years old. LOCRC cases were paired with EOCRC cases according to sex and tumor location. The exclusion criteria for both groups included having existing inflammatory bowel disease, histological diagnoses other than adenocarcinoma, and premalignant lesions/carcinomas *in situ*. All samples were collected before starting treatment, at the time of diagnosis. To rule out MSI status of the tumor, the presence of DNA mismatch repair (MMR) system deficiency was determined by immunohistochemistry, identifying the loss of the expression of any of the proteins MLH1, MSH2, MSH6, and PMS2 (22). To exclude hereditary forms, whole exome sequencing was performed, confirming that the microsatellite-stable (MSS) EOCRC cases analyzed were sporadic. Clinical and sociodemographic characteristics were collected for all participants.

2.2 Ethical statement

All individuals gave informed written consent to participate in the study before giving the blood sample. Protocol for this study (PIC 012-21-IIS-FJD) was prepared in accordance with the Helsinki Declaration and previously reviewed and approved by the Ethics Committee of Hospital Universitario Fundación Jiménez Díaz in Madrid (Spain). Current Spanish and European Data Protection Acts secured the confidentiality and anonymity of all participants.

2.3 Sample collection and processing

Blood samples were collected at the time of diagnosis before starting any treatment, either surgical or chemotherapy. The blood was immediately processed by centrifugation in a Ficoll-Hypaque density gradient (Corning, NY, USA) to isolate peripheral blood mononuclear cells (PBMCs) and plasma. After Ficoll separation, PBMCs were counted, assessed for viability, and cryopreserved at $\approx 10\times10^6$ cells/mL in freezing medium (90% heat-inactivated FBS + 10% DMSO) using a controlled-rate cooling device (≈–1 °C/min ramp) before transfer to the vapor phase of liquid nitrogen for long-term storage. All assays were performed after a single freeze–thaw cycle. Thawing was carried out rapidly at 37 °C, followed by gradual dilution in pre-warmed culture medium and a short resting period before stimulation or phenotyping. To minimize batch effects, paired EOCRC–LOCRC samples were processed and analyzed in parallel whenever possible.

2.4 Cell lines

K562 cell line (ECACC 89121407) was generously provided by Dr Cristina Eguizabal (Basque Center of Transfusions and Human Tissues, Álava, Spain). Raji cell line (ECACC 85011429) was provided by the existing collection of the Instituto de Salud Carlos III (Madrid, Spain). Both cell lines were cultured in RPMI medium enriched with 10% fetal bovine serum (FBS), 100U/ml of penicillin/streptomycin, and 2mM of L-Glutamin (Lonza, Basel, Switzerland).

2.5 Immune phenotyping and quantification of cytokine production by CD4+ T helper subpopulations

To measure cytokines produced by CD4+ T helper (Th) cell subsets, PBMCs were stimulated with phorbol 12-myristate 13-acetate (PMA) (25ng/ml) and ionomycin (1.5µg/ml) for 4h at 37°C in the presence of brefeldin A (BD GolgiPlug, BD Biosciences) to block exocytotic transport through the Golgi complex, allowing the expressed cytokines to remain inside the cell (23). Cells were then stained with the following conjugated antibodies: CD3-PE, CD8-APCH7, CXCR3-BV421, CCR4-PECy7, CCR6-BV650, and CCR10-BUV395. CD4+ Th subsets (CD3+CD8-) were

phenotyped according to the following patterns: Th1 (CXCR3+CCR6-), Th2 (CCR4+CCR6-), Th17 (CCR4+CCR6+), Th9 (CCR4-CCR6+), and Th22 (CCR4+CCR6+CCR10+). CD8+ T cells were also stained with the degranulation marker CD107a-PECy7 (BD Biosciences). After fixation and permeabilizing with IntraPrep Permeabilization Reagent (Immunostep, Salamanca, Spain), cells were intracellularly stained with the following antibodies to quantify the production of specific cytokines: IFNγ-FITC (Beckman Coulter, Brea, CA), IL4-APC, IL9-PercP, IL13-BV711, IL17a-BV510, and IL22-AF647 (BD Biosciences). Flow cytometry data were acquired using an LSRFortessa X-20 flow cytometer (BD Biosciences), and data analysis was performed using FlowJo v10.8 software (TreeStar Inc., Ashland, OR). The gating strategies used for the analysis of CD4+ Th subsets and their cytokine expression profiles are shown in Supplementary Figures 1 and 2, respectively.

2.6 Immune phenotyping of regulatory T cells

Regulatory T cells (Tregs) with the phenotype CD4+CD25+highCD127+low were characterized in PBMCs by flow cytometry using the following conjugated antibodies: CD4-PercP, CD25-PECy5, and CD127-FITC (BD Biosciences, San Jose, USA). Flow cytometry data acquisition and analysis were performed as described above.

2.7 Characterization of T-cell immune exhaustion and senescence

PBMCs were stained with Live/Dead Fixable Blue Dead Cell Stain Kit to discard dead cells and the following conjugated antibodies: CD3-NY660, CD4-BUV615, CD8a-NY730 (Thermo Fisher Scientific, Waltham, MA) to identify CD8+ and CD4+ T cells. Immune markers were stained as follows: senescence, CD57-PECyN7 and KLRG1-SB702; and exhaustion, PD1-SB780, LAG3-SB645, TIGIT-AF700, and TIM3-APC (Thermo Fisher Scientific). Flow cytometry data were acquired using a Cytek Aurora flow cytometer and SpectroFlo software (Cytek Biosciences, Fremont, CA), and data analysis was performed using FlowJo v10.8 software (TreeStar Inc.). The gating strategy used for the analysis of CD4+ and CD8+ T cell immune senescence and exhaustion is shown in Supplementary Figure 3.

2.8 Immune phenotyping and quantification of cytokine production by NK and NKT-like cells

NK and NKT-like cells, with the phenotype CD3-CD56+ and CD3+CD56+, respectively, were phenotyped based on the expression of activation and inhibition markers on their cell surface, using the following antibodies (BD Biosciences): inhibitory receptors, NKG2A-PE and CD158f-BV421; activating receptors, NKG2C-AF700, NKG2D-PECy7, NKp44-BUV395, and NKp46-BV650.

To measure cytokines produced by NK and NKT-like cells, PBMCs were stimulated with 1μg/ml of Hsp70 peptide (Abcam, Cambridge, UK) at 37°C in the presence of Brefeldin A (BD Biosciences) for 4 hours. Cells were then stained with the following conjugated antibodies: CD3-APC, CD56-BV605, CD16-BV421, CD107a-PECy7, and TCRγδ-BUV395. After fixation and permeabilization with IntraPrep Permeabilization Reagent (Immunostep), cells were intracellularly stained with IFNγ-PE (Beckman Coulter, Brea, CA), TNFα-PE, and Granzyme B (GZB)-FITC (BD Biosciences). Flow cytometry data acquisition and analysis were performed as described above. The gating strategy used for the phenotyping of NK and NKT cells and their cytokine expression profiles is shown in Supplementary Figure 4. The gating strategy to analyze CD8+ T cells and Tgd cells is shown in Supplementary Figure 5.

2.9 Measurement of capacity for direct cellular cytotoxicity of NK cells

Direct cellular cytotoxicity (DCC) of NK cells was measured as previously reported (24) using K562 cell line as missing-self target cells (25). K562 cells were stained with PKH26 Red Fluorescence Cell Linker kit (Sigma Aldrich-Merck) and then co-cultured for 1 hour at 37°C with PBMCs (1:1). Cells were then collected and Annexin V conjugated with FITC (Thermo Fisher) was used to measure early apoptosis by flow cytometry in stained K562 cells using an LSRFortessa X-20 flow cytometer (BD Biosciences). Data analysis was performed using FlowJo V10.8 software (TreeStar Inc.).

2.10 Measurement of glucose uptake in immune cell populations

To measure the capacity of PBMCs to uptake glucose, cells were incubated in glucose-deficient RPMI medium for 2h at 37°C. The fluorescent derivative of D-glucose monomer 2-[N-(7-nitrobenz-2-oxa-1,3-diazol-4-yl)amino]-2-deoxy-d-glucose (2-NBDG) (26), was added to the culture medium and incubated for 10 min at 37°C. Antibody against GLUT-1 conjugated with AF647 (BD Biosciences) was used to evaluate the expression of this marker. Flow cytometry data were acquired using an LSRFortessa X-20 flow cytometer (BD Biosciences), and data analysis was performed using FlowJo v10.8 software (TreeStar Inc.). The gating strategy used for the analysis of 2-NBDG probe uptake and Glut-1 expression is shown in Supplementary Figure 6.

2.11 Cytokine and chemokine levels in plasma

A custom 21-plex Human Magnetic Luminex Assay kit (R&D Systems, Minnesota, USA) was used to quantify the following

cytokines in plasma samples: pro-inflammatory, IL-1α, IL-1β, IL-6, IL12p70, IL-17, IFNβ, IFNγ, and TNFα; anti-inflammatory, IL-1RA, IL-4, and IL-10; chemokines, CCL2/MCP-1, CCL3/MIP-1α, CCL4/MIP-1β, CCL13/MCP-4, CCL20/MIP-3α, CCL23/MPIF, CXCL8/IL-8, and CXCL9/MIG; regulatory or homeostatic, IL-2, IL-7, and IL-15. A Luminex 200 system was used to acquire and analyze results using xPONENT software (Thermo Fisher Scientific).

2.12 Principal component analysis

Linear dimensionality reduction was performed using principal component analysis (PCA) (27) to capture the global structure of the data by finding the directions that maximize variance in the data. Python 3.11 was used with Pandas (28) for data import, NumPy (29) for numerical operations, Scikit-learn (30) for data normalization (in range [0, 1]) of continuous variables, and one-hot encoding for categorical features. Only parameters showing statistical significance ($p<0.05$) in univariate testing were analyzed. A biplot illustrating group clusters was generated with Matplotlib (31).

2.13 Random forest

A Random Forest algorithm (32) was applied to predict the categorization of participants with EOCRC or LOCRC and evaluate the resulting accuracy. The selection of these parameters was performed according to the existence of significant statistical differences between groups ($p<0.05$). To avoid bias in the selection of training, testing and validation sets, we performed a combined feature selection and classification procedure using a Random Forest classifier with a nested 5-fold cross-validation procedure for each competing algorithm, as previously described (33, 34). The relative importance for each feature in the categorization of participants with EOCRC or LOCRC was calculated by the Gini VIM method (35).

2.14 Statistical analysis

Statistical analysis was performed with GraphPad Prism v10.2.1 (GraphPad Software Inc.) and STATA 14.2 software (StataCorp LLC, College Station, TX). Samples' normal distribution was tested using the Shapiro-Wilk test. Quantitative variables were described as the median and interquartile range (IQR) and qualitative variables as absolute or relative frequencies. Qualitative data were compared by Fisher´s exact test, and quantitative data using the student's t-test or Mann-Whitney U test, as appropriate. Associations between qualitative clinical data and age of CRC development were assessed using binary logistic regression analysis (odds ratio, OR) and 95% confidence interval (CI). Associations between quantitative parameters and age of CRC development were determined using simple and logistic regressions to estimate the OR and CI, comparing LOCRC data as reference versus EOCRC data. To analyze data correlation and compute the Spearman coefficient r between all Th subsets per CRC cohort and within each cohort, we applied a combination of Python libraries such as Scikit-Learn (36) and Pandas (28, 37). For the generation of regression plots, the Seaborn library was used (38). Values of $p<0.05$ were considered statistically significant in all comparisons.

3 Results

3.1 Study population

This observational study recruited two cohorts of participants with CRC stratified by age (n=38). Sociodemographic and clinical descriptions of the participants are summarized in Table 1 and described in more detail in Supplementary Table 1. The EOCRC cohort had a median age of 44 years (IQR 41-48), while the LOCRC cohort had a median age of 76 years (IQR 55-84). Over half of the participants in both cohorts were men (63.2% in EOCRC and 52.6% in LOCRC). In all analyses, samples from men and women were identified separately to determine whether sex-related differences may exist in any of the assessed parameters with potential influence on the development of CRC.

Most participants presented with tumors in the left colon (36.8% in EOCRC and 42.1% in LOCRC), predominantly at stage III (31.6% in EOCRC and 36.8% in LOCRC), with no statistically significant differences between cohorts. Five participants in EOCRC cohort (26.3%) presented stage IV versus none in LOCRC cohort. MSI analysis revealed loss of protein expression in 3 participants (15.8%) in the EOCRC cohort, while none was observed in the LOCRC cohort. Family history of CRC was assessed only in EOCRC cases and showed that 52.6% were classified as sporadic. Whole exome sequencing confirmed that the MSS EOCRC cases included in our analyses were not associated with known hereditary CRC syndromes, ensuring that the comparisons reflect sporadic EOCRC versus LOCRC.

Comorbidities at the time of cancer diagnosis were more frequent in the LOCRC cohort (89.5% vs. 42.1% in EOCRC), with hypertension and heart conditions being the most prevalent (52.6% and 26.3%, respectively). Similarly, 84.2% of participants in the LOCRC cohort were undergoing medical treatment at the time of sampling, compared to 36.8% in the EOCRC cohort, with antihypertensive medication being the most common treatment in LOCRC (42.1%).

A binary logistic regression analysis was performed to evaluate whether demographic, clinical, and treatment variables were associated with the occurrence of EOCRC. None of these variables reached statistical significance, except for treatment with anticoagulants, which was associated with a higher odds ratio (OR = 10.50; 95% CI = 1.14–96.58; p=0.038) (Supplementary Table 2).

10.3389/fimmu.2025.1692382

3.2 Levels of CD4+ T cells and expression of dysfunction markers were similar between cohorts

We found no significant differences in the levels of total lymphocytes (CD3+), CD4+ T cells, or Tregs between the EOCRC and LOCRC cohorts (Figure 1A). Similarly, the expression of immune senescence markers (CD57 and KLRG1) and exhaustion markers (PD-1, LAG-3, TIGIT, and TIM-3) in CD4 + T cells did not differ significantly between cohorts (Figure 1B).

3.3 Enhanced functionality of CD4+ Th1 and Th2 cells in EOCRC participants

The levels of CD4+ Th1 cells were comparable between the EOCRC and LOCRC cohorts (Figure 2A, left graph). No significant differences were observed in the levels of IFNγ produced by these cells (Figure 2A, center graph); however, 40% of participants in the LOCRC cohort had CD4+ Th1 cells that were unable to produce IFNγ, compared to 15.8% in the EOCRC cohort (p=0.0001) (Figure 2A, right graph).

Similarly, CD4+ Th2 cell levels were comparable between the cohorts (Figure 2B, left graph), as were the levels of IL-4 and IL-13 produced by these cells (Figure 2B, center graphs). Nevertheless, 41.2% of LOCRC participants had Th2 cells with a reduced capacity to produce IL-4, compared to 15.8% in EOCRC (p<0.0001). Likewise, 31.6% of LOCRC participants and 15.8% of EOCRC participants showed a reduced capacity to produce IL-13 (p=0.0111) (Figures 2B, right graphs).

The calculation of Spearman's correlation between both cohorts in the levels of CD4+ Th1 and Th2 and representative cytokines produced by these cells showed no significant correlation between groups (Supplementary Figure 7A). However, within the EOCRC cohort, there was a moderate negative Th1/Th2 correlation (r=-0.45; p=0.05) (Supplementary Figure 7B), while this expected inverse association was absent in LOCRC (Supplementary Figure 7C).

3.4 Enhanced Th9/Th17 cytokine production but reduced Th22 cell levels in EOCRC

The levels of CD4+ Th9 cells were comparable between the EOCRC and LOCRC cohorts (Figure 3A, left graph), but cells from EOCRC participants produced significantly higher levels of IL-9 than those of the LOCRC cohort (2.5-fold; p=0.0356) (Figure 3A, center graph). Notably, 31.3% of LOCRC participants had Th9 cells that were unable to produce IL-9, compared to 15.8% in the EOCRC cohort (Figure 3A, right graph).

Similarly, CD4+ Th17 cell levels did not differ between the cohorts (Figure 3B, left graph), nor did the levels of IL-22 produced by these cells; however, Th17 cells from participants of EOCRC produced higher levels of IL-17A than LOCRC (4.8-fold; p=0.0374) (Figure 3B, center graphs). Moreover, a reduced capacity to produce IL-17A was observed in Th17 cells from 92.2% of LOCRC participants, compared to 61.1% in EOCRC (p<0.0001). Likewise, 92.2% of LOCRC participants and 77.8% of EOCRC participants showed impaired IL-22 production (p=0.0043) (Figures 3B, right graphs).

TABLE 1 Sociodemographic and clinical data of all participants in the study.

	EOCRC (n=19)	LOCRC (n=19)	P value
Age at cancer diagnosis, years; median (IQR)	44 (41–48)	76 (55–84)	**<0.0001**
Sex; n. male (%)	12 (63.2)	10 (52.6)	0.7431
Cancer location			
Right colon, n. (%)	5 (26.4)	6 (31.6)	1
Left colon, n. (%)	7 (36.8)	8 (42.1)	1
Rectum, n. (%)	7 (36.8)	5 (26.3)	0.7281
Stage			
I, n. (%)	3 (15.8)	5 (26.3)	0.6928
II, n. (%)	5 (26.3)	7 (36.8)	0.7281
III, n. (%)	6 (31.6)	7 (36.8)	1
IV, n. (%)	5 (26.3)	0 (0)	**0.0463**
Microsatellite instability, n. (%)	3 (15.8)	0 (0)	0.2297
CRC family history			
FDR, n. (%)	7 (36.8)	Unk.	–
SDR, n. (%)	2 (10.5)	Unk.	–
Sporadic, n. (%)	10 (52.6)	Unk.	–
Main comorbidities			
DM, n. (%)	2 (10.5)	4 (21.1)	0.6599
DL, n. (%)	2 (10.5)	4 (21.1)	0.6599
HTN, n. (%)	0 (0)	10 (52.6)	**0.0004**
Heart conditions, n. (%)	0 (0)	5 (26.3)	**0.0463**
Respiratory conditions, n. (%)	2 (10.5)	4 (21.1)	0.6599
Main treatment at sample collection			
Lipid lowering medication, n. (%)	2 (10.5)	7 (36.8)	0.1245
Anticoagulants, n. (%)	1 (5.3)	7 (36.8)	**0.0422**
Antihypertensive medication, n. (%)	0 (0)	8 (42.1)	**0.0031**
Diabetes medication, n. (%)	2 (10.5)	3 (15.8)	1

CRC, Colorectal cancer; DM, Diabetes mellitus; DL, Dyslipidemia; FDR, First degree relative; HTN, Hypertension; IQR, Interquartile Range; SDR, Second degree relative; Unk., Unknown. Fisher´s exact test was used to calculate statistical differences between cohorts. Significant p-values are highlighted in bold.

10.3389/fimmu.2025.1692382

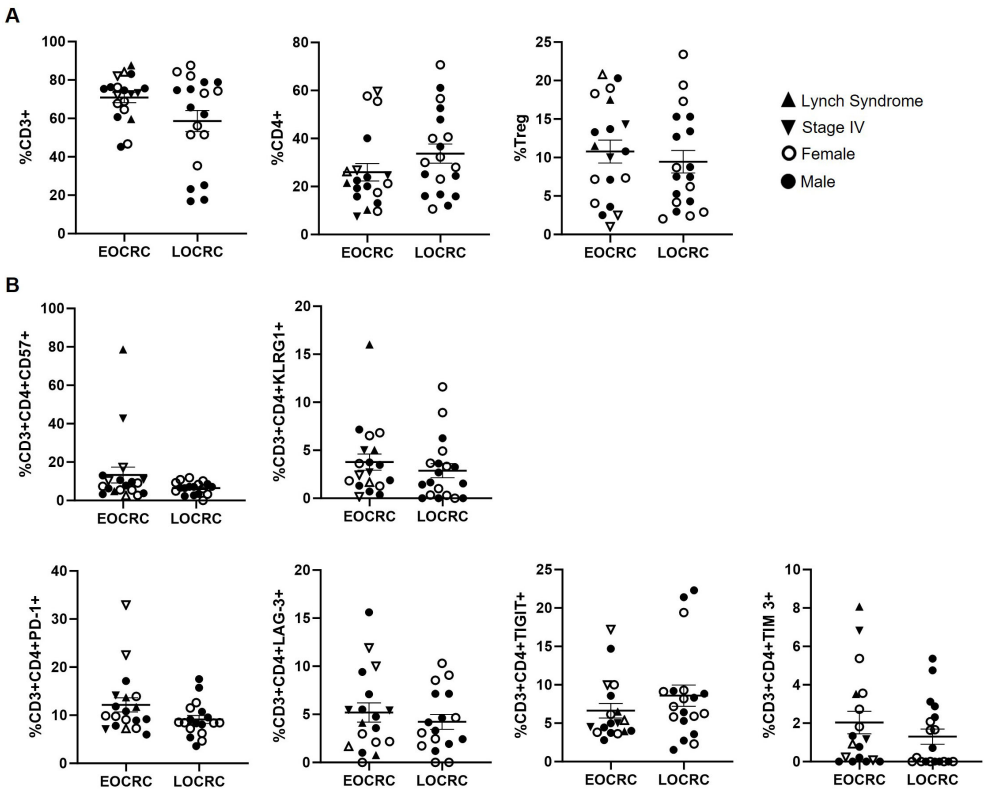

FIGURE 1
Peripheral blood CD4+ T cell composition and immune aging markers in EOCRC and LOCRC participants. **(A)** Levels of total T cells (CD3+), CD4+ T cells, and Tregs in peripheral blood of EOCRC and LOCRC participants. **(B)** Expression of immune senescence markers and exhaustion markers in CD4+ T cells from the participants. Each symbol corresponds to one sample and vertical lines represent the standard error of the mean (SEM). Open symbols correspond to EOCRC and closed symbols correspond to LOCRC. Upright closed triangles indicate participants with Lynch syndrome and inverted closed triangle indicate participants with stage IV. Statistical analysis was performed with Mann-Whitney test or Unpaired t test as appropriate.

CD4+ Th22 cell levels were 2.4-fold lower in EOCRC participants compared to those in LOCRC (p=0.0133) (Figure 3C, left graph). In contrast, IL-13 levels produced by these cells were 4-fold higher compared to LOCRC (p=0.0310), while IL-22 production did not differ significantly between cohorts (Figure 3C, center graphs). However, impaired IL-13 production was observed in Th22 cells from 75% of LOCRC participants, compared to 50% in EOCRC (p = 0.0004). Similarly, 80% of LOCRC participants and 61.1% of EOCRC participants showed reduced IL-22 production capacity (p=0.0050) (Figures 3C, right graphs).

The calculation of Spearman's correlation between both cohorts in the levels of CD4+ Th9, Th17, and Th22 and representative cytokines produced by these cells showed no significant correlation between groups (Supplementary Figure 7A). There was a significant negative association between Th9 and Th22 in the EOCRC cohort (r = -0.53, p = 0.02) (Supplementary Figure 7B), contrasted by distinct patterns in LOCRC: a significant negative correlation between Th1 and Th22 (r = -0.55, p = 0.02), a borderline association between Th2 and Th9 (r = -0.44, p = 0.06), and a moderate positive correlation between Th17 and Th22 (r = 0.49, p = 0.05) (Supplementary Figure 7C).

3.5 CD8+ T cells from EOCRC showed similar levels to LOCRC but higher LAG-3 expression

No differences were observed between cohorts in CD8+ T cell levels or in their degranulation capacity, assessed by CD107a expression (Figure 4A). The analysis of immune senescence and exhaustion markers in these cells revealed a significantly higher expression of the exhaustion marker LAG-3 in EOCRC participants, with a 1.5-fold increase compared to LOCRC (p=0.0255) (Figure 4B).

3.6 Reduction of CD8+ Tγδ cells in EOCRC with preserved degranulation capacity

CD8+ Tγδ cell levels were 2.9-fold lower in EOCRC compared to LOCRC (p=0.0073), while CD107a expression in these cells was similar between cohorts (Figure 5A). No differences were observed between cohorts in the levels of CD8- Tγδ cells or in their CD107a expression (Figure 5B).

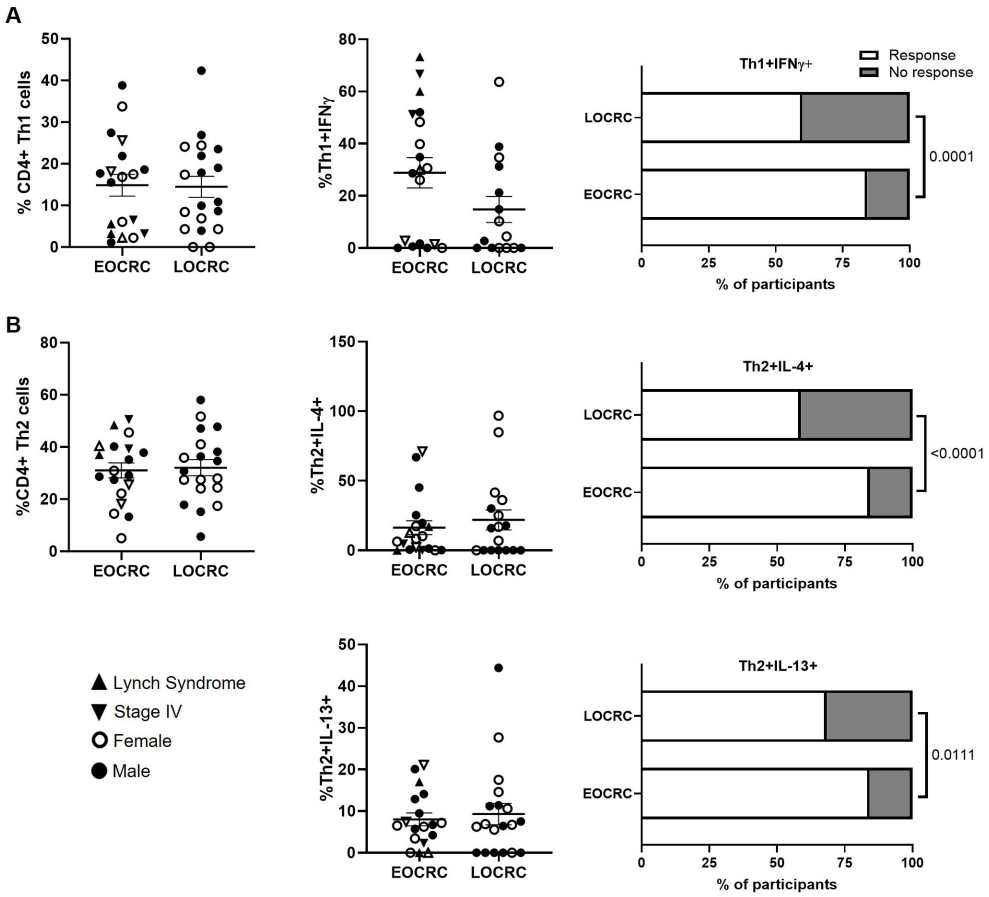

FIGURE 2
Functional profiling of peripheral CD4+ Th1 and Th2 cells in EOCRC and LOCRC participants. **(A)** Frequency of CD4+ Th1 cells in peripheral blood of EOCRC and LOCRC and levels of IFNγ produced by these cells. **(B)** Frequency of CD4+ Th2 cells and levels of IL-4 and IL-13 produced by these cells. Bar graphs on the right represent the percentage of cells able to produce each cytokine. Open symbols correspond to EOCRC and closed symbols correspond to LOCRC. Upright closed triangles indicate participants with Lynch syndrome and inverted closed triangle indicate participants with stage IV. Statistical analysis was performed with Mann-Whitney test or Unpaired t test as appropriate. Fisher´s exact test was used to calculate significance between cohorts in horizontal bar graphs.

3.7 Higher NKT-like cell levels in EOCRC with comparable functionality

NKT-like cell levels were 2.5-fold higher in EOCRC compared to LOCRC (p=0.0288) (Figure 6A, left graph). However, no differences were observed in their degranulation capacity (Figure 6A, right graph) or in cytokine production in response to Hsp70 peptides (Figure 6B).

3.8 NK cells in EOCRC showed similar phenotypic profiles but reduced cytotoxic capacity

NK cell levels and their degranulation capacity were similar between cohorts (Figure 7A). Although there were no significant differences in the levels of cytokines produced by these cells in response to Hsp70 peptides (Figure 7B, left graphs), a proportion of EOCRC participants presented NK cells lacking the capacity to produce IFNγ (5.3%, p=0.0289) and TNFα (15.8%; p<0.0001) (Figure 7B, right graphs). The capacity of these cells to exert direct cellular cytotoxicity (DCC) against K562 target cells was 2.0-fold reduced in EOCRC compared to LOCRC (p=0.0438) (Figure 7C).

We found no differences between groups in the expression of inhibitory or activating markers on the NK cell surface (Supplementary Figure 8).

3.9 Higher glucose uptake in EOCRC PBMCs with unchanged GLUT-1 expression

PBMCs from EOCRC participants showed 1.8-fold higher glucose uptake than LOCRC (p=0.0152), as measured using the glucose analog 2-NBDG (Figure 8A). No differences between cohorts were observed in the expression levels of GLUT-1 transporter (Figure 8B).

10.3389/fimmu.2025.1692382

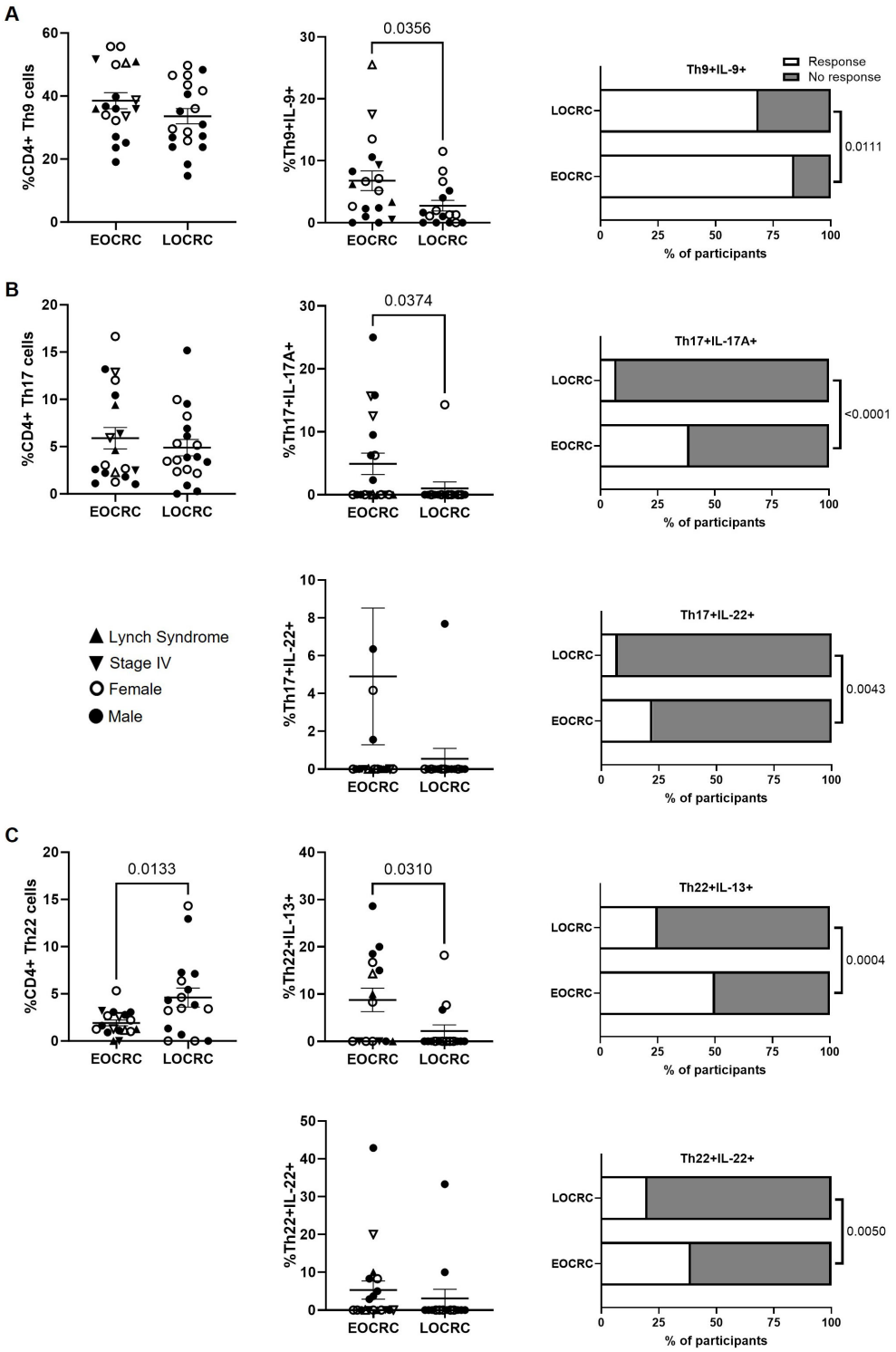

FIGURE 3
Functional profiling of peripheral CD4+ Th9, Th17, and Th22 cells in EOCRC and LOCRC participants. **(A)** Frequency of CD4+ Th9 cells in peripheral blood of EOCRC and LOCRC and levels of IL-9 produced by these cells. **(B)** Frequency of CD4+ Th17 cells and levels of IL-17A and IL-22 produced by these cells. **(C)** Frequency of CD4+ Th22 cells and levels of IL-13 and IL-22 produced by these cells. Bar graphs on the right represent the percentage of cells able to produce each cytokine. Open symbols correspond to EOCRC and closed symbols correspond to LOCRC. Upright closed triangles indicate participants with Lynch syndrome and inverted closed triangle indicate participants with stage IV. Statistical analysis was performed with Mann-Whitney test or Unpaired t test as appropriate. Fisher´s exact test was used to calculate significance between cohorts in horizontal bar graphs.

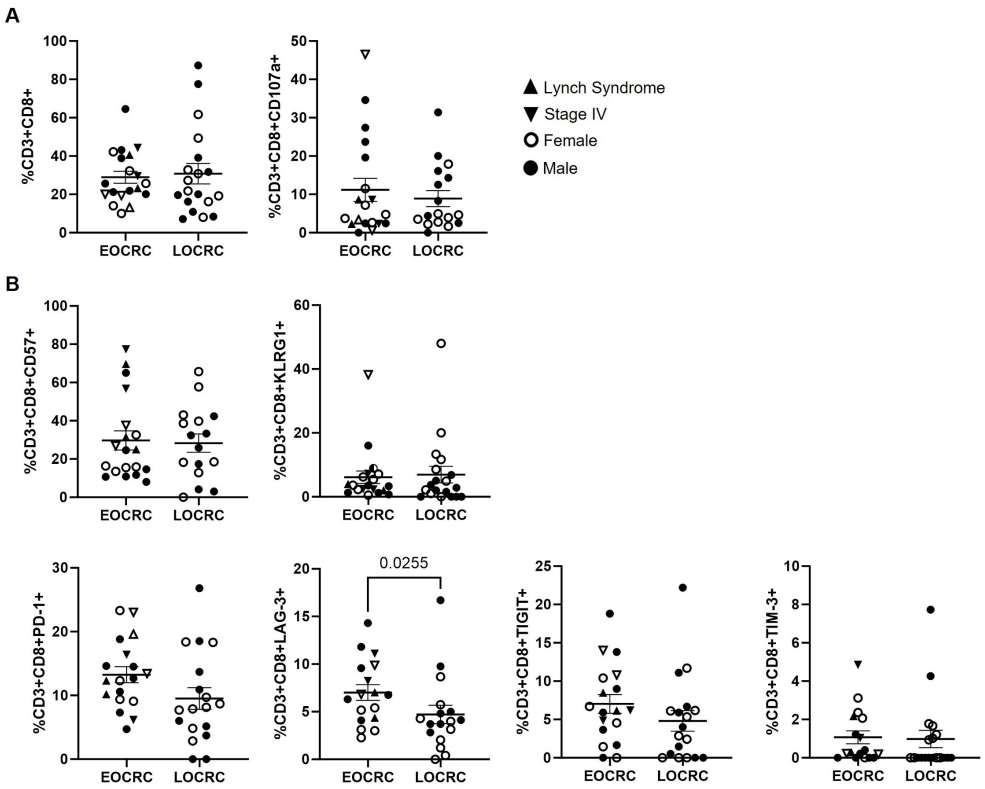

FIGURE 4
Peripheral blood CD8+ T cell composition and immune aging markers in EOCRC and LOCRC participants. **(A)** Levels of total CD8+ T cells (left graph) and expression of the degranulation marker CD107a (right graph) in peripheral blood of EOCRC and LOCRC participants. **(B)** Expression of immune senescence markers and exhaustion markers in CD8+ T cells from the participants. Each symbol corresponds to one sample and vertical lines represent the standard error of the mean (SEM). Open symbols correspond to EOCRC and closed symbols correspond to LOCRC. Upright closed triangles indicate participants with Lynch syndrome and inverted closed triangle indicate participants with stage IV. Statistical analysis was performed with Mann-Whitney test or Unpaired t test as appropriate.

3.10 Increased systemic inflammatory markers IFNγ and IL-8/CXCR8 in EOCRC

Plasma cytokine analysis revealed significantly higher levels of IFNγ (23-fold; p=0.0284) and CXCR8/IL-8 (3.2-fold; p= 0.0162) in EOCRC participants compared to LOCRC, along with lower levels of CCL13/MCP-4 (-1.7-fold; p=0.0208) (Figure 9).

3.11 Distinct immunometabolic profiling signatures differentiated EOCRC from LOCRC

PCA revealed a partial separation between EOCRC and LOCRC participants along the first principal component (PCA1) (Figure 10A). Although there was some overlap, most EOCRC samples clustered on the left side of the PCA1 axis, while LOCRC samples displayed a broader distribution across both PCA1 and PCA2 axes. These results suggest that the multivariate immune parameters contributing to PCA1, potentially related to immune, metabolic, or molecular parameters, differed between both cohorts, with EOCRC individuals exhibiting a more homogeneous profile.

To assess whether immunological and metabolic parameters could discriminate between EOCRC and LOCRC, we trained a Random Forest classifier using selected variables. The model achieved a mean cross-validation accuracy of 90.0% (± 14.6%) across five folds (Figure 10B), with a confusion matrix showing high classification performance: 94.7% accuracy for EOCRC and 84.2% for LOCRC (Figure 10C). The most informative features contributing to classification were counts of CD4+ Th22 cells, CD8 + Tγδ cells, and CD8+ T cells expressing the exhaustion marker LAG-3, as well as plasma levels of CCL13/MCP-4 (Figure 10D). These results suggested that a distinct immunometabolic signature can effectively distinguish between EOCRC and LOCRC.

3.12 Immunological predictors of risk for EOCRC

Most of the discriminative features identified by the random forest model were corroborated by binary logistic regression, which identified four parameters with significant predictive value (Supplementary Table 3): CD4+ Th22 cells (β=0.0638, OR = 1.5012, p=0.034), CD8+ TCRγδ+ cells (β=0.0479, OR = 1.4861,

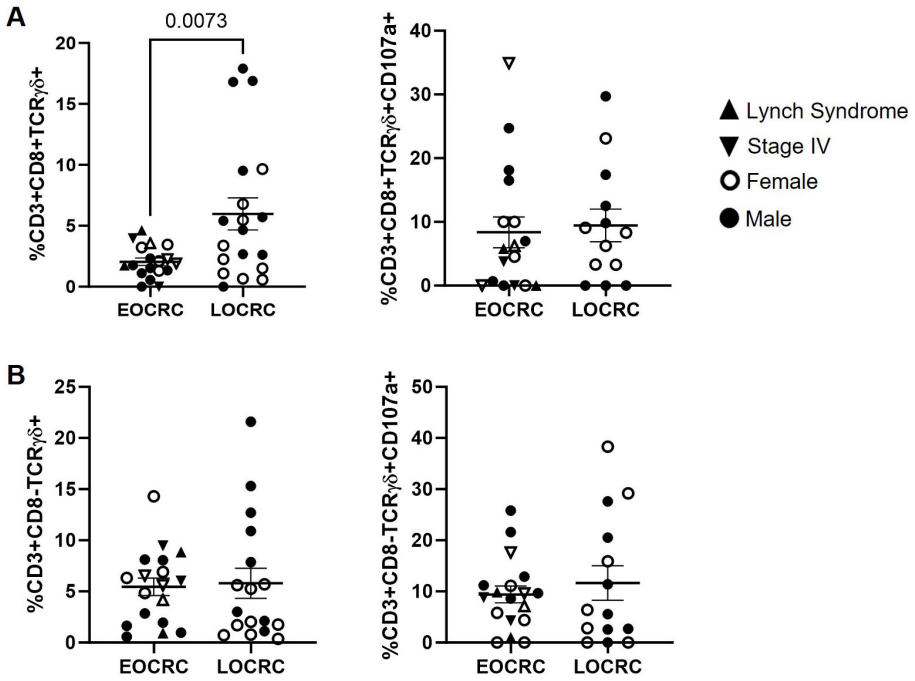

FIGURE 5
Peripheral blood Tγδ cell levels and expression of CD107a in EOCRC and LOCRC participants. Levels of CD8+ **(A)** and CD8- **(B)** Tγδ cells (left graphs) and expression of the degranulation marker CD107a in these cells (right graphs) in peripheral blood of EOCRC and LOCRC participants. Each symbol corresponds to one sample and vertical lines represent the standard error of the mean (SEM). Open symbols correspond to EOCRC and closed symbols correspond to LOCRC. Upright closed triangles indicate participants with Lynch syndrome and inverted closed triangle indicate participants with stage IV. Statistical analysis was performed with Mann-Whitney test or Unpaired t test as appropriate.

p=0.035), IL-13 produced by Th22 cells (β=-0.0250, OR = 0.8835, p=0.044), and NKT-like cells (β=-0.0060, OR = 0.9722, p=0.019).

4 Discussion

CRC remains a leading cause of cancer-related death worldwide. While screening programs have successfully reduced incidence in older adults, the occurrence of EOCRC has risen sharply over the past decades (12, 39), challenging paradigms and fundamental biological differences between age-stratified diseases. The tissue-based Immunoscore has proven a superior predictor of disease-free and overall survival compared to the conventional TNM (Tumor Nodes Metastasis) staging system (40). However, because it relies on postoperative tumor specimens, its utility is limited to prognosis after diagnosis rather than prevention or early detection. Whether the immune determinants of prognosis identified in tumor tissue are reflected in peripheral blood, and whether they differ fundamentally between EOCRC and LOCRC, remains unexplored. This study addresses these questions by comprehensively profiling circulating immune landscapes in age-stratified CRC cohorts to identify biomarkers suitable for a minimally invasive liquid Immunoscore.

In our study, CRC participants were stratified by age into EOCRC and LOCRC, without statistically significant differences between cohorts in cancer stages I-III, location, or MSI. Notably, five EOCRC individuals had stage IV disease versus none in the LOCRC cohort. Although this imbalance could confound immune-profile comparisons, these five stage-IV cases did not cluster separately in any of our analyses, indicating that the immune signatures we identified are driven by age-related factors rather than metastatic burden. Whole exome sequencing confirmed that the MSS EOCRC cases included in our analyses were not associated with known hereditary CRC syndromes, ensuring that the comparisons presented here reflect sporadic EOCRC versus LOCRC. Additionally, even though 89.5% of LOCRC participants presented comorbidities versus 42.1% of EOCRC participants, and most LOCRC participants were taking medication to treat these comorbidities, these percentages were similar to those observed in the general population for this age group (41, 42). Furthermore, although we considered sex in the analysis of each parameter, no clear pattern emerged to suggest that sex plays a major role in the development of EOCRC. This was further supported by the odds ratio analysis, which indicated that sex was not associated with an increased risk. These findings validate that the distinct immune landscapes we report are genuine age-associated phenomena rather than artefacts of clinical confounders.

Total peripheral blood immune cell counts such as CD3+, CD4+, and regulatory T cells, as well as markers of T-cell senescence/exhaustion in total CD4+ populations, did not differ between EOCRC and LOCRC cohorts. However, functional assays revealed an increased capacity to produce cytokines from the

10.3389/fimmu.2025.1692382

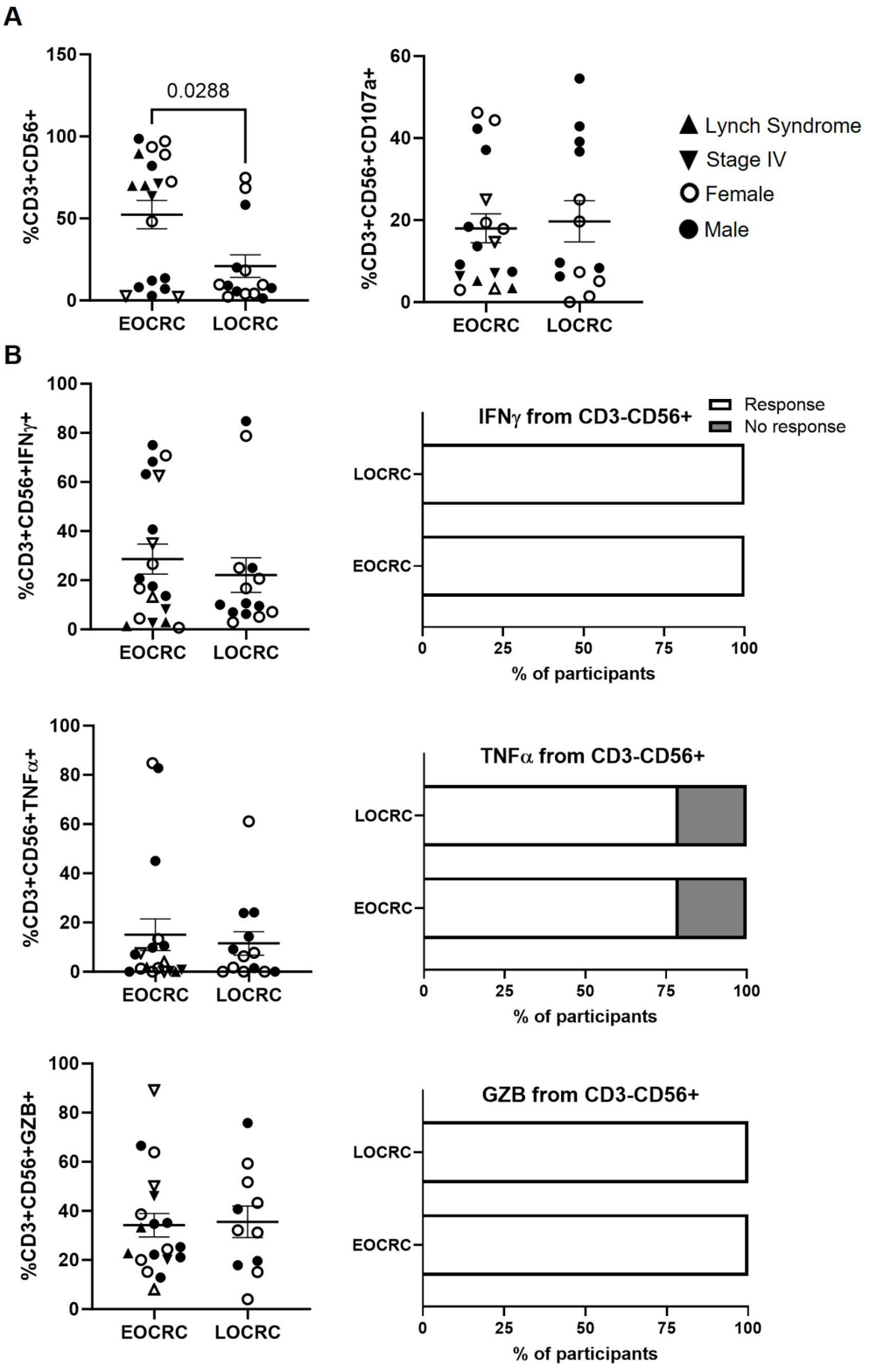

FIGURE 6
Functional profiling of peripheral NKT-like cells in EOCRC and LOCRC participants. **(A)** Levels of NKT-like cells in peripheral blood of EOCRC and LOCRC and expression of CD107a in these cells. **(B)** Levels of IFNγ, TNFα, and GZB produced by NKT-like cells. Bar graphs on the right represent the percentage of cells able to produce each cytokine. Open symbols correspond to EOCRC and closed symbols correspond to LOCRC. Upright closed triangles indicate participants with Lynch syndrome and inverted closed triangle indicate participants with stage IV. Statistical analysis was performed with Mann-Whitney test or Unpaired t test as appropriate. Fisher´s exact test was used to calculate significance between cohorts in horizontal bar graphs.

10.3389/fimmu.2025.1692382

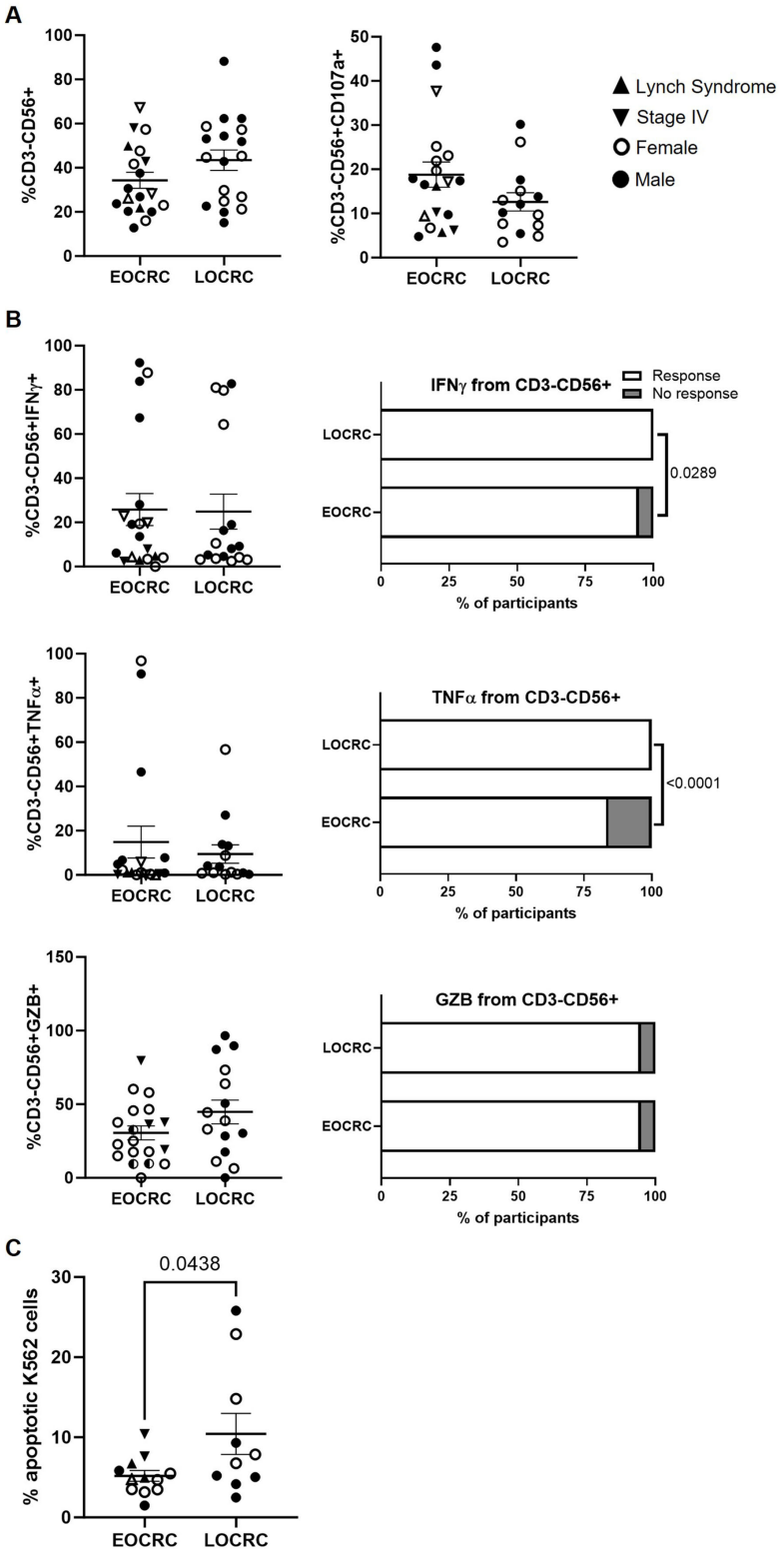

FIGURE 7
Functional profiling of peripheral NK cells in EOCRC and LOCRC participants. **(A)** Levels of NK cells in peripheral blood of EOCRC and LOCRC and expression of CD107a in these cells. **(B)** Levels of IFNγ, TNFα, and GZB produced by NK cells. Bar graphs on the right represent the percentage of cells able to produce each cytokine. **(C)** Percentage of K562 cells in apoptosis after co-culture with PBMCs from the participants. Open symbols correspond to EOCRC and closed symbols correspond to LOCRC. Upright closed triangles indicate participants with Lynch syndrome and inverted closed triangle indicate participants with stage IV. Statistical analysis was performed with Mann-Whitney test or Unpaired t test as appropriate. Fisher´s exact test was used to calculate significance between cohorts in horizontal bar graphs.

10.3389/fimmu.2025.1692382

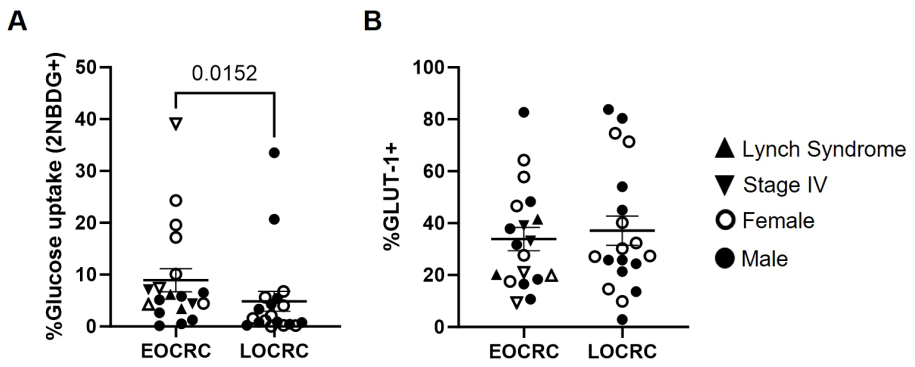

FIGURE 8
Glucose uptake and GLUT-1 expression in PBMCs from EOCRC and LOCRC participants. Percentage of uptake of the glucose analog 2-NBDG by PBMCs from the participants **(A)** and expression of GLUT-1 receptor on the surface of these cells **(B)**. Open symbols correspond to EOCRC and closed symbols correspond to LOCRC. Upright closed triangles indicate participants with Lynch syndrome and inverted closed triangle indicate participants with stage IV. Statistical analysis was performed with Mann-Whitney test or Unpaired t test as appropriate.

different CD4+ Th subsets in participants with EOCRC, who also presented a distinctly more proinflammatory Th1/Th9/Th17 profile. This functional activation pattern, rather than reflecting immune decline, is consistent with the immune profile typically observed in younger individuals, characterized by stronger Th polarization and preserved naïve/memory balance (43). Such features may indicate that EOCRC arises in a proinflammatory systemic milieu, whereas LOCRC reflects features of immunosenescence and "inflammaging," with reduced adaptive flexibility and impaired effector function (44).

An adequate CD4+ Th cell polarization is essential for the appropriate coordination of cellular and humoral responses against pathogens or cancer cells (45, 46), and each subset contributes differently to tumor progression. In CRC, a preferential polarization to Th1 intracellular response is generally assumed to promote prolonged disease-free survival (47–49), mostly due to their capacity to produce IFNγ that may activate an efficient response against intracellular challenges (50). CD4+ Th1 cells from EOCRC participants showed higher capacity to produce IFNγ, whose plasma levels were significantly increased compared to the LOCRC cohort. This finding contrasts with previous reports (49) and studies in advanced CRC showing impaired IFNγ responses associated with immune exhaustion and tumor progression. Importantly, our EOCRC cohort, despite including five stage IV cases, maintained robust IFNγ production, suggesting that age-related immune competence may override stage-dependent exhaustion mechanisms in younger patients. This is further supported by recent single-cell analyses, which show that younger patients retain higher proportions of functional effector T cells, even in advanced disease stages (51). These results suggested that the immune response of younger participants could be better at controlling tumor progression. In fact, the classical, mutually inhibitory Th1/Th2 axis was only preserved in EOCRC participants, thereby reflecting intact IFNγ-mediated suppression of Th2 differentiation (52). However, the absence of significantly negative correlation in LOCRC indicates that aging may disrupt the normal balance between opposing Th cell subpopulations.

CD4+ Th17 subset has been associated with tumor progression by inducing IL-17-mediated angiogenesis, suppressing CD8+ TILs, and thereby promoting a worse prognosis (49, 53–55). However, Th17 cells may also recruit neutrophils and CD8+ T cells directly via chemokines like CXCL8/IL-8, which has been linked to better CRC outcomes (56). Therefore, Th17 cells may present a dual role in CRC (56). Our EOCRC participants showed higher capacity to produce IL-17A from Th17 cells than LOCRC, which aligns with studies describing inflammatory mucosal signatures and Th17-enriched microenvironments in early-onset tumors (57), along with higher plasma levels of CXCL8/IL-8. This profile might reflect an inflammatory but ineffective immune response, insufficient for full elimination of tumor cells yet capable of promoting angiogenesis and early tumor growth. Conversely, LOCRC patients exhibited elevated plasma levels of CCL13/MCP-4, a chemokine involved in the recruitment of monocytes, eosinophils, and Th2-skewed lymphocytes that mediate tissue remodeling and chronic inflammation (58), likely reflecting a pro-remodeling, Th2-biased immune environment consistent with immunosenescence and inflammaging. The concurrent decrease in IFNγ and IL-8 further supports a defective Th1-mediated effector function and impaired inflammatory signaling, indicating a shift from protective anti-tumor immunity toward chronic, dysregulated inflammation. This cytokine signature is in line with inflammaging processes that favor tissue repair and remodeling over immune clearance, thereby potentially facilitating tumor persistence in LOCRC.

Similarly, CD4+ Th9 cells have also shown a dual effect on tumors (59), presenting anti-tumorigenic effects in most cancers (60, 61), but able to promote CRC in colitis-associated neoplasm models (62). The frequencies of Th9 cells in the CRC tumor positively correlate with the rates of CD8+ TILs (63). Although we did not observe significant differences between cohorts in the Th9 cell count, these cells expressed higher levels of IL-9 in EOCRC participants than LOCRC. Due to IL-9 may amplify IL-17-driven inflammation and angiogenesis (64) and stimulate both Th17 activity and CXCL8/IL-8 production (65), this cytokine strongly

10.3389/fimmu.2025.1692382

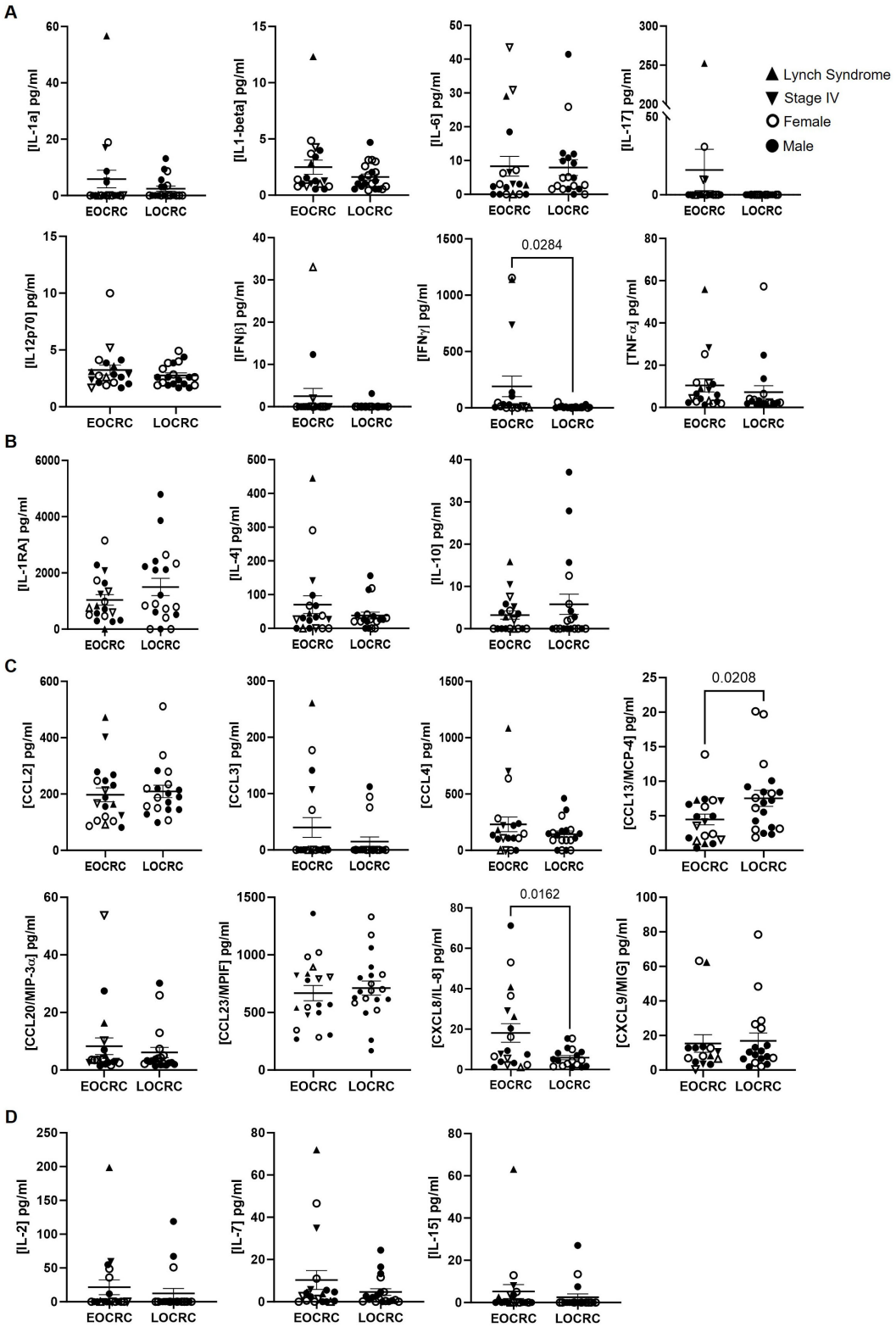

FIGURE 9
Plasma cytokine levels in EOCRC and LOCRC participants. Levels of pro-inflammatory **(A)**, anti-inflammatory **(B)**, chemotactic **(C)**, and homeostatic **(D)** cytokines in plasma of the participants. Open symbols correspond to EOCRC and closed symbols correspond to LOCRC. Upright closed triangles indicate participants with Lynch syndrome and inverted closed triangle indicate participants with stage IV. Statistical analysis was performed with Mann-Whitney test or Unpaired t test as appropriate.

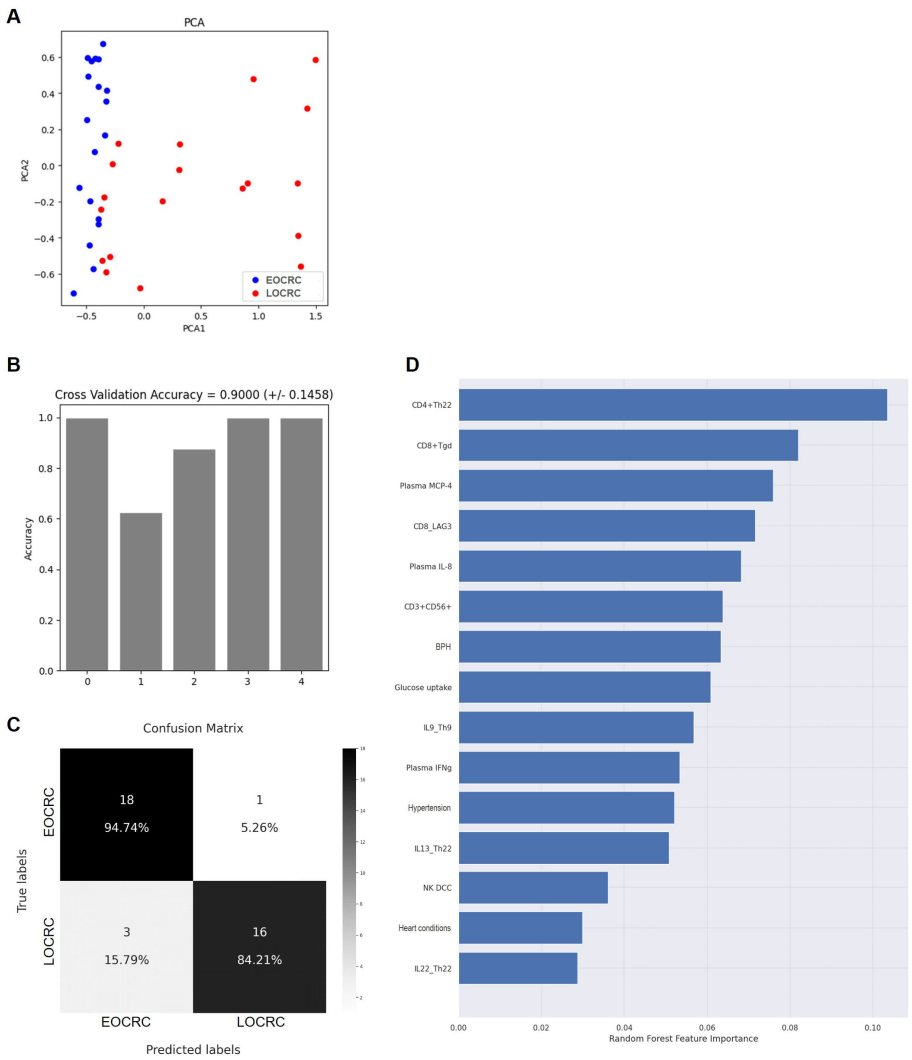

FIGURE 10
PCA visualization and random forest-based classification performance and feature importance of selected immune biomarkers. **(A)** PCA-based visualization showing separation of EOCRC and LOCRC participants. **(B)** Classification accuracy across 5 outer iterations of nested K-fold cross-validation using a random forest model. **(C)** Confusion matrix comparing predicted and actual diagnostic categories (EOCRC vs. LOCRC). **(D)** Relative importance of selected biomarkers for classification based on the Gini variable importance measure. BPH, Benign prostatic hyperplasia; DCC, Direct cellular cytotoxicity; IFNγ, Interferon gamma; LAG-3, Lymphocyte-activation gene 3; MCP-4, Monocyte chemoattractant protein-4.

contributes to the general pro-inflammatory environment observed in EOCRC participants. This coordinated upregulation of IL-9 and IL-17A may indicate a proangiogenic, early inflammatory state favoring tumor initiation, as suggested in models of colitis-associated CRC (66). Conversely, LOCRC patients, with higher IL-13-producing Th22 cells, exhibited a reparative, senescent-like immune signature potentially associated with chronic inflammation and tissue remodeling rather than acute immune activation (67).

Finally, the levels of CD4+ Th22 cells were significantly reduced in our EOCRC cohort. These cells are characterized by the production of IL-22 and also exhibit a dual role in CRC, acting in tissue repair in both early-stage disease and tumor progression as the inflammation becomes chronic (68). IL-22 has been involved in mucosal defense, tissue repair, and wound healing (69), but also with CRC tumor progression through the activation of the STAT3 pathway, promoting cancer cell self-renewal and tumorigenesis (70). Intriguingly, while Th22 frequencies were reduced in EOCRC, these cells showed enhanced per-cell capacity to produce both IL-22 and IL-13 compared to LOCRC. This functional enhancement despite numerical reduction suggests a compensatory activation phenotype, where fewer cells attempt to maintain tissue homeostasis under inflammatory stress. The elevated IL-13 production by Th22 cells in EOCRC is particularly notable, as IL-13 is typically produced by CD4+ Th2 cells, involved in promoting tissue remodeling and fibrosis (71). The elevated production of IL-13 by Th22 cells in EOCRC patients suggests a potential shift in their functional profile, which together with their reduced levels, may promote a proinflammatory environment with

an impaired capacity for tissue repair and immune regulation in EOCRC, potentially leading to unchecked tumor progression. However, Th22 cells also showed enhanced capacity to produce IL-22 and IL-13 in EOCRC, which could promote aggressive tumor behavior and shape an immunosuppressive environment favorable to tumor survival and growth (72). In contrast, LOCRC patients exhibited an accumulation of Th22 cells with impaired capacity to produce IL-22, which supported a dysregulated immune response that may contribute to chronic inflammation and tumor development. This pattern aligns with findings showing that aged immune systems accumulate phenotypically defined but functionally exhausted cell subsets (73), contributing to chronic inflammation without effective tissue repair, a state conducive to tumor development and progression.

Moreover, Th9/Th22 correlation was negative in EOCRC cohort, suggesting that IL-9-driven inflammatory signals may help restrain IL-22-mediated STAT3 activation and tumor-promoting self-renewal pathways (62, 74). By contrast, LOCRC participants exhibited a broad reduction in cytokine production across multiple Th subsets, highlighted by negative Th1/Th22 and Th2/Th9 correlations, as well as a positive Th17/Th22 correlation, thereby pointing at a functional decline in adaptive immunity. This altered polarization may reflect immunosenescent and inflammaging phenotypes characterized by skewing toward IL-22/IL-17-driven tissue repair and chronic inflammation (68, 72, 75). Consistent with our observation of a higher proportion of non-IFNγ-producing Th1 and reduced cytokine production in Th2 cells in LOCRC, age-associated declines in type-1 T cell function and reduced IFNγ production have been repeatedly documented in older individuals (76, 77). These changes reflect hallmarks of immunosenescence in LOCRC and are associated with reduced adaptive immunity and chronic, low-grade inflammation.

Additionally, LOCRC participants showed higher frequency of CD8+ Tγδ cells that under chronic inflammatory or senescent conditions may adopt regulatory or tissue-repair functions instead of exerting direct cytotoxic activity against tumor cells (78). This suggests that despite the preserved numbers, the cytotoxic potential of these cells is functionally compromised in LOCRC, contributing to impaired tumor immunosurveillance and a shift toward a pro-remodeling, chronic inflammatory microenvironment. Collectively, cytotoxic cell phenotype and CD4+ Th subset interactions may imply that EOCRC pathogenesis involves a failure of immune elimination despite preserved regulatory pathways and increased levels of NKT-like cells in peripheral blood, which was supported by the reduced cytotoxic capacity of NK cells and likely NKT cells, and by increased levels of exhausted LAG3+ CD8+ T cells. However, LOCRC seems to arise from progressive immune decline induced by inflammaging and loss of tumor immunosurveillance, illustrated by an overall consistent impaired functional and metabolic capacity in the immune cells. Specifically, the combination of higher regulatory-like CD8+ Tγδ cells and reduced NK/NKT cytotoxicity reflects a functional decline in the effector arm of immunity, pointing to a mechanistic link between immunosenescence and reduced anti-tumor activity in older patients.

In our study, PBMCs from EOCRC patients displayed higher glucose uptake than those from LOCRC, despite no differences in GLUT-1 expression. This observation may indicate a global enhancement of metabolic activity among circulating mononuclear cells. Previous studies have shown that immune activation and systemic inflammation are accompanied by metabolic remodeling of PBMCs, including increased glycolytic flux and altered mitochondrial function in diverse settings (79, 80), and systemic inflammatory responses have been documented in CRC (81). Moreover, studies measuring circulating immune bioenergetics in cancer patients indicate that PBMC metabolic phenotypes can reflect disease-associated immune states (82). We speculate that the increased metabolic activity of immune cells in EOCRC may favor the emergence of highly glycolytic tumor clones, potentially contributing to their more aggressive clinical behavior. In contrast, LOCRC PBMCs showed reduced metabolic activity, which may limit cytokine production and cytotoxic responses, contributing to chronic inflammation and tissue-remodeling milieu characteristic of immunosenescence.

Feature importance analysis ranked Th22 cell frequency, CD8+ Tγδ cells, plasma CCL13/MCP-4, and LAG3+ CD8+ T cells as the top contributors to age-based CRC stratification. These findings were corroborated by binary logistic regression, which indicated that decreased frequencies of Th22 cells and CD8+ Tγδ cells were risk factors for EOCRC, suggesting an altered proinflammatory environment with functionally compromised immune responses that fail to contain early tumor progression. Conversely, higher IL-13 production by Th22 cells and increased circulating NKT-like cells were protective factors for EOCRC, indicating compensatory immunoregulatory and innate-like antitumor activity more prominent in early-onset disease. In contrast, LOCRC participants exhibited broader variation across these immune-metabolic parameters, consistent with immunosenescence, reduced cytotoxic capacity, and impaired effector function.

The main limitation of this study was that although peripheral blood is an accessible source for immune monitoring, circulating immune phenotypes may not fully represent the tumor microenvironment, where local immune landscape and cell-cell interactions may modulate effector function. Therefore, further integrating tumor microenvironment analyses would be necessary to deepen understanding of these systemic immune alterations.

In conclusion, our findings revealed distinct immunological profiles characterizing EOCRC versus LOCRC. EOCRC presented a heightened proinflammatory environment with altered functionality but retaining compensatory regulatory pathways. In contrast, LOCRC exhibited features consistent with immunosenescence and inflammaging, with impaired cytokine production and a shift toward tissue-remodeling and chronic inflammation pathways. These findings highlight the potential to incorporate differential biomarkers such as frequencies and functional states of Th22 cells, CD8+ Tγδ cells, IL-13 production, and NKT-like cells into a liquid Immunoscore based on peripheral blood analysis. Unlike classical Immunoscore, which relies on postoperative tumor tissue and serves primarily a prognostic role, a liquid Immunoscore would offer a minimally invasive, accessible tool with preventive capabilities. This

could enable early immune-based risk stratification and detection of CRC, particularly in younger populations at risk for EOCRC, facilitating timely and personalized immunotherapeutic interventions to improve clinical outcomes. Further studies with larger cohorts would be needed to ensure the validity of the approach.

Data availability statement

The original contributions presented in the study are included in the article/Supplementary Material. Further inquiries can be directed to the corresponding authors.

Ethics statement

The studies involving humans were approved by Ethics Committee of Hospital Universitario Fundación Jiménez Díaz, Madrid (Spain). The studies were conducted in accordance with the local legislation and institutional requirements. The participants provided their written informed consent to participate in this study.

Author contributions

MC: Supervision, Methodology, Data curation, Investigation, Conceptualization, Validation, Writing – review & editing, Project administration, Writing – original draft, Formal Analysis, Funding acquisition. CS-M: Writing – original draft, Investigation, Formal Analysis, Writing – review & editing, Methodology. JR-P: Writing – review & editing, Formal Analysis, Methodology, Investigation. DF: Investigation, Software, Writing – review & editing, Formal Analysis, Methodology. VL: Writing – review & editing, Methodology, Investigation. MG-S: Writing – review & editing, Investigation, Methodology. EM: Methodology, Investigation, Supervision, Writing – review & editing. MC: Investigation, Data curation, Writing – review & editing, Formal Analysis. EJ: Writing – review & editing, Investigation, Resources. GS: Writing – review & editing, Investigation, Resources. EÁ: Resources, Writing – review & editing, Investigation. AB-P: Writing – review & editing, Investigation, Resources. MM-G: Investigation, Writing – review & editing, Resources. JR: Resources, Investigation, Writing – review & editing. EH-C: Resources, Writing – review & editing, Investigation. CP: Investigation, Resources, Writing – review & editing. FB: Resources, Writing – review & editing, Investigation. AS: Investigation, Resources, Writing – review & editing. JM-L: Writing – review & editing, Investigation, Data curation, Methodology, Formal Analysis. MT: Investigation, Writing – original draft, Methodology, Formal Analysis, Project administration, Writing – review & editing, Data curation, Supervision. JP: Investigation, Methodology, Validation, Formal Analysis, Funding acquisition, Supervision, Writing – review & editing, Project administration, Conceptualization, Writing – original draft, Resources.

Group members of the Spanish EOCRC consortium

José A. Alcazar[1], Oscar Alonso[2], Carlos Álvarez Laso[3], Edgardo Celi Altamarina[4], Alicia Alvarellos[5], Edurne Álvaro[6], Jorge Arredondo[5], María Arriba Domenech[7], Francesc Balaguer[8,9,10,11], Araceli Ballestero[14], Javier Barambio[6], Francisco Blanco Antona[1], Lorena Brandáriz[6], Ana Burdaspal[6], Sabela Carballal[8,9,10,11], Joaquín Castillo[8,9,10,11], Adriana Cavero[12], Cristian Cisterne[4], Gonzalo Colmenarejo[13], Miriam Cuatrecasas[8,9,10,11], María Daca-Alvarez[8,9,10,11], Javier Die Trill[14], Jana Dziakova[2], Isabel Espinosa-Salinas[13], Lidia Estudillo[15], Lara P. Fernández[13], Alba Fernández Candela[16], José M. Fernández Cebrián[14], Daniel Fernández Martínez[3], María Luisa de Fuenmayor[6], Leire García Alonso[3], Luis García Florez[3], Elena García García[4], Juan L. García[17], Damián García-Olmo[18], Ariadna García-Rodríguez[19], Marta Gómez de Cedrón[13], Rogelio González-Sarmiento[17], Pablo Granero Castro[3], Pol Guarner Piquet[20], Sergio Hernández-Villafranca[18], Elena Hurtado[7], Fernando Jiménez Escovar[12], Luis M. Jiménez Gómez[7], Marta Jiménez Toscano[21], Miquel Kraft[19], Hardeep Kumari[8,9,10,11], Ignacio Hevia Lorenzo[3], Ana B. Herrero[17], Mar Iglesias Coma[21], Irene López Rojo[2], Carmen Martínez Sánchez[20], Núria Malats[15], Franco Marinello[19], Marc Martí[19], Ignacio Matos[5], Leticia Moreira[8,9,10,11], Lorena Moreno[8,9,10,11], Paula Munoz Munoz[16], Juan Ocana Jiménez[14], Teresa Ocana[8,9,10,11], Ma del Mar Pardo[4], Carlos Pastor[5], Isabel Peligros Gómez[6], María Pellisé[8,9,10,11], José Perea[17,23], Sara Picazo Marín[22], Vicente Portugal[12], Jésica Pérez[17], Ana Ramírez de Molina[13], Javier Rodríguez[5], José I. Rodríguez García[3], José A. Rueda Orgaz[4], Gonzalo Sanz[22], Rodrigo Sanz López[22], Ariadna Sánchez[8,9,10,11], Aida Suárez Álvarez[3], María Suárez Solís[22], Ana Teijo[2], Nuria Truan Alonso[3], Laura Vega López[4], Rosario Vidal Tocino[1], Ignacio Valverde[24], Cristina Viyuela[24], Jaime Zorrilla Ortúzar[7].

[1]Salamanca University Hospital, Salamanca, Spain

[2]MD Anderson Cancer Center Spain, Madrid, Spain

[3]Central de Asturias University Hospital, Oviedo, Spain

[4]Fundación Hospital Alcorcón, Alcorcón, Madrid, Spain

[5]Navarra University Clinic (Clínica Universidad de Navarra), Pamplona, Navarra, Spain

[6]Infanta Leonor University Hospital, Madrid, Spain

[7]Gregorio Maranón University Hospital, Madrid, Spain

[8]Department of Gastroenterology, Hospital Clınic de Barcelona, Barcelona, Spain

[9]Institut d'Investigacions Biomediques August Pi i Sunyer (IDIBAPS), Barcelona, Spain

[10]Centro de Investigación Biomédica en Red de Enfermedades Hepáticas y Digestivas (CIBEREHD), Barcelona, Spain

[11]University of Barcelona, Barcelona, Spain

[12]Galdakao-Usansolo Hospital, Galdakao, Vizcaya, Spain

[13]Molecular Oncology IMDEA Food Institute, Madrid, Spain

[14]Ramón y Cajal University Hospital, Madrid, Spain

[15]Spanish National Cancer Research Center (CNIO), Genetic & Molecular Epidemiology Group, Madrid, Spain

[16]Quirónsalud Torrevieja Hospital, Torrevieja, Alicante, Spain

[17]Biomedical Research Institute of Salamanca (IBSAL), Salamanca, Spain

[18]Fundación Jiménez Díaz University Hospital, Madrid, Spain
[19]Vall d'Hebron University Hospital, Barcelona, Spain
[20]Hospital de la Santa Creu i Sant Pau. Barcelona, Spain
[21]Hospital del Mar, Barcelona, Spain
[22]Hospital Universitario Clínico San Carlos, Madrid, Spain
[23]Vithas Arturo Soria University Hospital, Madrid, Spain
[24]Villalba University Hospital, Madrid, Spain

Funding

The author(s) declare financial support was received for the research and/or publication of this article. This work was funded by Strategic Action in Health of the Instituto de Salud Carlos III (ISCIII) (grant PI20/0974 and PI24/0729) (co-funded by European Regional Development Fund 'A way to make Europe'); the Spanish Ministry of Science and Innovation, grant PID2022-141317OB-I00 funded by MICIU/AEI/10.13039/501100011033 and the European Regional Development Fund (ERDF), EU; and CIBERINFEC (Centro de Investigación Biomédica en Red Enfermedades Infecciosas), group CB21/13/00015, Instituto de Salud Carlos III, Ministerio de Ciencia e Innovación and Unión Europea – NextGenerationEU. The work of CS-M is financed by a pre-doctoral grant funded by the Community of Madrid (CAM), Spain (PIPF-2023_SAL-GL-30376). The work of VL is supported by a pre-doctoral grant from Instituto de Salud Carlos III (ISCIII-PFIS FI24/00326). The work of Montserrat Torres is financed by CIBERINFEC (CB21/13/00015).

Acknowledgments

We greatly appreciate all individuals who participated in this study. We also thank the physicians who contributed with the recruitment of the participants and the collection of blood samples.

Conflict of interest

The authors declare that the research was conducted in the absence of any commercial or financial relationships that could be construed as a potential conflict of interest.

Generative AI statement

The author(s) declare that no Generative AI was used in the creation of this manuscript.

Any alternative text (alt text) provided alongside figures in this article has been generated by Frontiers with the support of artificial intelligence and reasonable efforts have been made to ensure accuracy, including review by the authors wherever possible. If you identify any issues, please contact us.

Publisher's note

Supplementary material

The Supplementary Material for this article can be found online at: https://www.frontiersin.org/articles/10.3389/fimmu.2025.1692382/full#supplementary-material

References

1. Bray F, Laversanne M, Sung H, Ferlay J, Siegel RL, Soerjomataram I, et al. Global cancer statistics 2022: GLOBOCAN estimates of incidence and mortality worldwide for 36 cancers in 185 countries. *CA Cancer J Clin*. (2024) 74(3):229–63. doi: 10.3322/caac.21834

2. Sullivan BA, Noujaim M, Roper J. Cause, epidemiology, and histology of polyps and pathways to colorectal cancer. *Gastrointest Endosc Clin N Am*. (2022) 32:177–94. doi: 10.1016/j.giec.2021.12.001

3. *Cancer Facts & Figures 2023*. Atlanta: American Cancer Society, Inc. (2022). Available online at: https://www.cancer.org/research/cancer-facts-statistics/all-cancer-facts-figures/2023-cancer-facts-figures.html.

4. Montminy EM, Zhou M, Maniscalco L, Abualkhair W, Kim MK, Siegel RL, et al. Contributions of adenocarcinoma and carcinoid tumors to early-onset colorectal cancer incidence rates in the United States. *Ann Intern Med*. (2021) 174:157–66. doi: 10.7326/M20-0068

5. Siegel RL, Miller KD, Fedewa SA, Ahnen DJ, Meester RGS, Barzi A, et al. Colorectal cancer statistics, 2017. *CA Cancer J Clin*. (2017) 67:177–93. doi: 10.3322/caac.21395

6. Siegel RL, Torre LA, Soerjomataram I, Hayes RB, Bray F, Weber TK, et al. Global patterns and trends in colorectal cancer incidence in young adults. *Gut*. (2019) 68:2179–85. doi: 10.1136/gutjnl-2019-319511

7. Vuik FE, Nieuwenburg SA, Bardou M, Lansdorp-Vogelaar I, Dinis-Ribeiro M, Bento MJ, et al. Increasing incidence of colorectal cancer in young adults in Europe over the last 25 years. *Gut*. (2019) 68:1820–6. doi: 10.1136/gutjnl-2018-317592

8. Fritz CDL, Otegbeye EE, Zong X, Demb J, Nickel KB, Olsen MA, et al. Red-flag signs and symptoms for earlier diagnosis of early-onset colorectal cancer. *J Natl Cancer Inst*. (2023) 115:909–16. doi: 10.1093/jnci/djad068

9. Shapley M, Mansell G, Jordan JL, Jordan KP. Positive predictive values of ≥5% in primary care for cancer: systematic review. *Br J Gen Pract*. (2010) 60:e366–77. doi: 10.3399/bjgp10X515412

10. Burnett-Hartman AN, Lee JK, Demb J, Gupta S. An update on the epidemiology, molecular characterization, diagnosis, and screening strategies for early-onset colorectal cancer. *Gastroenterology*. (2021) 160:1041–9. doi: 10.1053/j.gastro.2020.12.068

11. Zhang F, Qiao S. Research progress on the relationship between inflammation and colorectal cancer. *Ann Gastroenterol Surg*. (2021) 6:204–11. doi: 10.1002/ags3.12517

12. Siegel RL, Jakubowski CD, Fedewa SA, Davis A, Azad NS. Colorectal cancer in the young: epidemiology, prevention, management. *Am Soc Clin Oncol Educ Book*. (2020) 40):e75–88. doi: 10.1200/EDBK_279901

13. Gupta S, Bharti B, Ahnen DJ, Buchanan DD, Cheng IC, Cotterchio M, et al. Potential impact of family history based screening guidelines on early onset colorectal cancer detection. *Cancer*. (2020) 126:3013–20. doi: 10.1002/cncr.32851

14. Terzić J, Grivennikov S, Karin E, Karin M. Inflammation and colon cancer. *Gastroenterology*. (2010) 138:2101–14. doi: 10.1053/j.gastro.2010.01.058

15. Simon K. Colorectal cancer development and advances in screening. *Clin Interv Aging*. (2016) 11:967. doi: 10.2147/CIA.S109285

16. Galon J, Costes A, Sanchez-Cabo F, Kirilovsky A, Mlecnik B, Lagorce-Pagès C, et al. Type, density, and location of immune cells within human colorectal tumors predict clinical outcome. *Science*. (2006) 313:1960–4. doi: 10.1126/science.1129139

17. Andric F, Al-Fairouzi A, Wettergren Y, Szeponik L, Bexe-Lindskog E, Cusack JC, et al. Immune microenvironment in sporadic early-onset versus average-onset colorectal cancer. *Cancers*. (2023) 15:1457. doi: 10.3390/cancers15051457

18. Kuznetsova O, Fedyanin M, Zavalishina L, Moskvina L, Kuznetsova O, Lebedeva A, et al. Prognostic and predictive role of immune microenvironment in colorectal cancer. *World J Gastrointest Oncol*. (2024) 16:643–52. doi: 10.4251/wjgo.v16.i3.643

19. Mlecnik B, Bindea G, Angell HK, Maby P, Angelova M, Tougeron D, et al. Integrative analyses of colorectal cancer show immunoscore is a stronger predictor of patient survival than microsatellite instability. *Immunity*. (2016) 44:698–711. doi: 10.1016/j.immuni.2016.02.025

20. Pagès F, Mlecnik B, Marliot F, Bindea G, Ou FS, Bifulco C, et al. International validation of the consensus Immunoscore for the classification of colon cancer: a prognostic and accuracy study. *Lancet Lond Engl*. (2018) 391:2128–39. doi: 10.1016/S0140-6736(18)30789-X

21. Perea J, Marti M, Espin E, Hernandez-Villafranca S, Orihuela P, Vidal Tocino R, et al. Cohort profile: the Spanish Early-onset Colorectal Cancer (SECOC) cohort: a multicentre cohort study on the molecular basis of colorectal cancer among young individuals in Spain. *BMJ Open*. (2021) 11:e055409. doi: 10.1136/bmjopen-2021-055409

22. Umar A, Boland CR, Terdiman JP, Syngal S, de la Chapelle A, Rüschoff J, et al. Revised bethesda guidelines for hereditary nonpolyposis colorectal cancer (Lynch syndrome) and microsatellite instability. *J Natl Cancer Inst*. (2004) 96:261–8. doi: 10.1093/jnci/djh034

23. Strous GJ, van Kerkhof P, van Meer G, Rijnboutt S, Stoorvogel W. Differential effects of brefeldin A on transport of secretory and lysosomal proteins. *J Biol Chem*. (1993) 268:2341–7. doi: 10.1016/S0021-9258(18)53781-9

24. Vigón L, Fuertes D, García-Pérez J, Torres M, Rodríguez-Mora S, Mateos E, et al. Impaired cytotoxic response in PBMCs from patients with COVID-19 admitted to the ICU: biomarkers to predict disease severity. *Front Immunol*. (2021) 12:665329. doi: 10.3389/fimmu.2021.665329

25. Pugh J, Nemat-Gorgani N, Djaoud Z, Guethlein LA, Norman PJ, Parham P. *In vitro* education of human natural killer cells by KIR3DL1. *Life Sci Alliance*. (2019) 2: e201900434. doi: 10.26508/lsa.201900434

26. Yamada K, Nakata M, Horimoto N, Saito M, Matsuoka H, Inagaki N. Measurement of glucose uptake and intracellular calcium concentration in single, living pancreatic beta-cells. *J Biol Chem*. (2000) 275:22278–83. doi: 10.1074/jbc.M908048199

27. Lever J, Krzywinski M, Altman N. Principal component analysis. *Nat Methods*. (2017) 14:641–2. doi: 10.1038/nmeth.4346

28. team T pandas development. pandas-dev/pandas: Pandas (2025). Zenodo. Available online at: https://zenodo.org/records/15597513.

29. Harris CR, Millman KJ, van der Walt SJ, Gommers R, Virtanen P, Cournapeau D, et al. Array programming with numPy. *Nature*. (2020) 585:357–62. doi: 10.1038/s41586-020-2649-2

30. Buitinck L, Louppe G, Blondel M, Pedregosa F, Mueller A, Grisel O, et al. European Conference on Machine Learning and Principles and Practices of Knowledge Discovery in Databases. (2013).

31. Hunter JD. Matplotlib: A 2D graphics environment. *Comput Sci Eng*. (2007) 9:90–5. doi: 10.1109/MCSE.2007.55

32. Breiman L. Random forests. *Mach Learn*. (2001) 45:5–32. doi: 10.1023/A:1010933404324

33. Meyer HV, Birney E. PhenotypeSimulator: A comprehensive framework for simulating multi-trait, multi-locus genotype to phenotype relationships. *Bioinformatics*. (2018) 34:2951–6. doi: 10.1093/bioinformatics/bty197

34. Sarica A, Cerasa A, Quattrone A. Random forest algorithm for the classification of neuroimaging data in alzheimer's disease: A systematic review. *Front Aging Neurosci*. (2017) 9:329. doi: 10.3389/fnagi.2017.00329

35. Nembrini S, König IR, Wright MN. The revival of the Gini importance? *Bioinformatics*. (2018) 34:3711–8. doi: 10.1093/bioinformatics/bty373

36. Pedregosa F, Varoquaux G, Gramfort A, Michel V, Thirion B, Grisel O, et al. Scikit-learn: machine learning in python. *arXiv*. (2018) 12:2825–30. Available online at: http://arxiv.org/abs/1201.0490.

37. McKinney W. Data structures for statistical computing in python. *Proc 9th Python Sci Conf*. (2010), 56–61. doi: 10.25080/issn.2575-9752

38. Waskom ML. seaborn: statistical data visualization. *J Open Source Software*. (2021) 6:3021. doi: 10.21105/joss.03021

39. Schmoll HJ, Van Cutsem E, Stein A, Valentini V, Glimelius B, Haustermans K, et al. ESMO Consensus Guidelines for management of patients with colon and rectal cancer. A personalized approach to clinical decision making. *Ann Oncol*. (2012) 23:2479–516. doi: 10.1093/annonc/mds236

40. Bruni D, Angell HK, Galon J. The immune contexture and Immunoscore in cancer prognosis and therapeutic efficacy. *Nat Rev Cancer*. (2020) 20:662–80. doi: 10.1038/s41568-020-0285-7

41. Salive ME. Multimorbidity in older adults. *Epidemiol Rev*. (2013) 35:75–83. doi: 10.1093/epirev/mxs009

42. Forjaz MJ, Rodriguez-Blazquez C, Ayala A, Rodriguez-Rodriguez V, de Pedro-Cuesta J, Garcia-Gutierrez S, et al. Chronic conditions, disability, and quality of life in older adults with multimorbidity in Spain. *Eur J Intern Med*. (2015) 26:176–81. doi: 10.1016/j.ejim.2015.02.016

43. Goronzy JJ, Weyand CM. Mechanisms underlying T cell ageing. *Nat Rev Immunol*. (2019) 19:573–83. doi: 10.1038/s41577-019-0180-1

44. Franceschi C, Garagnani P, Parini P, Giuliani C, Santoro A. Inflammaging: a new immune-metabolic viewpoint for age-related diseases. *Nat Rev Endocrinol*. (2018) 14:576–90. doi: 10.1038/s41574-018-0059-4

45. Kervevan J, Chakrabarti LA. Role of CD4+ T cells in the control of viral infections: recent advances and open questions. *Int J Mol Sci*. (2021) 22:523. doi: 10.3390/ijms22020523

46. Anaya J-M, Shoenfeld Y, Rojas-Villarraga A, Levy RA, Cervera R. *Autoimmunity: From bench to bedside*. Bogotá (Colombia): School of Medicine and Health Sciences, El Rosario University: El Rosario University Press (2013).

47. Pagès F, Kirilovsky A, Mlecnik B, Asslaber M, Tosolini M, Bindea G, et al. *In situ* cytotoxic and memory T cells predict outcome in patients with early-stage colorectal cancer. *J Clin Oncol*. (2009) 27:5944–51. doi: 10.1200/JCO.2008.19.6147

48. Bindea G, Mlecnik B, Tosolini M, Kirilovsky A, Waldner M, Obenauf AC, et al. Spatiotemporal dynamics of intratumoral immune cells reveal the immune landscape in human cancer. *Immunity*. (2013) 39:782–95. doi: 10.1016/j.immuni.2013.10.003

49. Tosolini M, Kirilovsky A, Mlecnik B, Fredriksen T, Mauger S, Bindea G, et al. Clinical impact of different classes of infiltrating T cytotoxic and helper cells (Th1, th2, treg, th17) in patients with colorectal cancer. *Cancer Res*. (2011) 71:1263–71. doi: 10.1158/0008-5472.CAN-10-2907

50. Camus M, Tosolini M, Mlecnik B, Pagès F, Kirilovsky A, Berger A, et al. Coordination of intratumoral immune reaction and human colorectal cancer recurrence. *Cancer Res*. (2009) 69:2685–93. doi: 10.1158/0008-5472.CAN-08-2654

51. Zhang L, Li Z, Skrzypczynska KM, Fang Q, Zhang W, O'Brien SA, et al. Single-cell analyses inform mechanisms of myeloid-targeted therapies in colon cancer. *Cell*. (2020) 181:442–59. doi: 10.1016/j.cell.2020.03.048

52. Romagnani S, Parronchi P, D'Elios MM, Romagnani P, Annunziato F, Piccinni MP, et al. An update on human th1 and th2 cells. *Int Arch Allergy Immunol*. (2009) 113:153–6. doi: 10.1159/000237532

53. Yoshida N, Kinugasa T, Miyoshi H, Sato K, Yuge K, Ohchi T, et al. A high RORγT/CD3 ratio is a strong prognostic factor for postoperative survival in advanced colorectal cancer: analysis of helper T cell lymphocytes (Th1, th2, th17 and regulatory T cells). *Ann Surg Oncol*. (2016) 23:919–27. doi: 10.1245/s10434-015-4923-3

54. Chen J, Chen Z. The effect of immune microenvironment on the progression and prognosis of colorectal cancer. *Med Oncol*. (2014) 31:82. doi: 10.1007/s12032-014-0082-9

55. Czajka-Francuz P, Cisoń-Jurek S, Czajka A, Kozaczka M, Wojnar J, Chudek J, et al. Systemic interleukins' Profile in early and advanced colorectal cancer. *Int J Mol Sci*. (2021) 23:124. doi: 10.3390/ijms23010124

56. Amicarella F, Muraro MG, Hirt C, Cremonesi E, Padovan E, Mele V, et al. Dual role of tumour-infiltrating T helper 17 cells in human colorectal cancer. *Gut*. (2017) 66:692–704. doi: 10.1136/gutjnl-2015-310016

57. Akimoto N, Ugai T, Zhong R, Hamada T, Fujiyoshi K, Giannakis M, et al. Rising incidence of early-onset colorectal cancer: a call for action. *Nat Rev Clin Oncol*. (2021) 18:230–43. doi: 10.1038/s41571-020-00445-1

58. Mendez-Enriquez E, García-Zepeda EA. The multiple faces of CCL13 in immunity and inflammation. *Inflammopharmacology*. (2013) 21:397–406. doi: 10.1007/s10787-013-0177-5

59. Chen J, Guan L, Tang L, Liu S, Zhou Y, Chen C, et al. T helper 9 cells: A new player in immune-related diseases. *DNA Cell Biol*. (2019) 38:1040–7. doi: 10.1089/dna.2019.4729

60. Nonomura Y, Otsuka A, Nakashima C, Seidel JA, Kitoh A, Dainichi T, et al. Peripheral blood Th9 cells are a possible pharmacodynamic biomarker of nivolumab treatment efficacy in metastatic melanoma patients. *Oncoimmunology*. (2016) 5: e1248327. doi: 10.1080/2162402X.2016.1248327

61. Lu Y, Wang Q, Xue G, Bi E, Ma X, Wang A, et al. Th9 cells represent a unique subset of CD4+ T cells endowed with the ability to eradicate advanced tumors. *Cancer Cell*. (2018) 33:1048–1060.e7. doi: 10.1016/j.ccell.2018.05.004

62. Gerlach K, Popp V, Wirtz S, Al-Saifi R, Gonzalez Acera M, Atreya R, et al. PU.1-driven th9 cells promote colorectal cancer in experimental colitis models through il-6 effects in intestinal epithelial cells. *J Crohns Colitis*. (2022) 16:1893–910. doi: 10.1093/ecco-jcc/jjac097

63. Wang C, Lu Y, Chen L, Gao T, Yang Q, Zhu C, et al. Th9 cells are subjected to PD-1/PD-L1-mediated inhibition and are capable of promoting CD8 T cell expansion through IL-9R in colorectal cancer. *Int Immunopharmacol*. (2020) 78:106019. doi: 10.1016/j.intimp.2019.106019

64. Singh TP, Schön MP, Wallbrecht K, Gruber-Wackernagel A, Wang XJ, Wolf P. Involvement of IL-9 in th17-associated inflammation and angiogenesis of psoriasis. *PloS One*. (2013) 8:e51752. doi: 10.1371/journal.pone.0051752

65. Midde HS, Priyadarssini M, Rajappa M, Munisamy M, Mohan Raj PS, Singh S, et al. Interleukin-9 serves as a key link between systemic inflammation and angiogenesis in psoriasis. *Clin Exp Dermatol*. (2021) 46:50–7. doi: 10.1111/ced.14335

66. Tanimura Y, Fukui T, Horitani S, Matsumoto Y, Miyamoto S, Suzuki R, et al. Long-term model of colitis-associated colorectal cancer suggests tumor spread mechanism and nature of cancer stem cells. *Oncol Lett*. (2021) 21:7. doi: 10.3892/ol.2020.12268

67. Zhou J, Tang Z, Gao S, Li C, Feng Y, Zhou X. Tumor-associated macrophages: recent insights and therapies. *Front Oncol*. (2020) 10:188. doi: 10.3389/fonc.2020.00188

68. Huang YH, Cao YF, Jiang ZY, Zhang S, Gao F. Th22 cell accumulation is associated with colorectal cancer development. *World J Gastroenterol WJG*. (2015) 21:4216–24. doi: 10.3748/wjg.v21.i14.4216

69. Ouyang W, O'Garra A. IL-10 family cytokines IL-10 and IL-22: from basic science to clinical translation. *Immunity*. (2019) 50:871–91. doi: 10.1016/j.immuni.2019.03.020

70. Doulabi H, Masoumi E, Rastin M, Foolady Azarnaminy A, Esmaeili SA, Mahmoudi M. The role of Th22 cells, from tissue repair to cancer progression. *Cytokine*. (2022) 149:155749. doi: 10.1016/j.cyto.2021.155749

71. Chiaramonte MG, Donaldson DD, Cheever AW, Wynn TA. An IL-13 inhibitor blocks the development of hepatic fibrosis during a T-helper type 2–dominated inflammatory response. *J Clin Invest*. (1999) 104:777–85. doi: 10.1172/JCI7325

72. Doulabi H, Rastin M, Shabahangh H, Maddah G, Abdollahi A, Nosratabadi R, et al. Analysis of Th22, Th17 and CD4+cells co-producing IL-17/IL-22 at different stages of human colon cancer. *BioMed Pharmacother*. (2018) 103:1101–6. doi: 10.1016/j.biopha.2018.04.147

73. Hearps AC, Martin GE, Angelovich TA, Cheng WJ, Maisa A, Landay AL, et al. Aging is associated with chronic innate immune activation and dysregulation of monocyte phenotype and function. *Aging Cell*. (2012) 11:867–75. doi: 10.1111/j.1474-9726.2012.00851.x

74. Kryczek I, Lin Y, Nagarsheth N, Peng D, Zhao L, Zhao E, et al. IL-22+CD4+ T cells promote colorectal cancer stemness via STAT3 transcription factor activation and induction of the methyltransferase DOT1L. *Immunity*. (2014) 40:772–84. doi: 10.1016/j.immuni.2014.03.010

75. Ling L, Zhao P, Yan G, Chen M, Zhang T, Wang L, et al. The frequency of Th17 and Th22 cells in patients with colorectal cancer at pre-operation and post-operation. *Immunol Invest*. (2015) 44:56–69. doi: 10.3109/08820139.2014.936445

76. Sutherland A, Cook A, Miller C, Duncan L, Yuecel R, Heys S, et al. Older patients are immunocompromised by cytokine depletion and loss of innate immune function after HIP fracture surgery. *Geriatr Orthop Surg Rehabil*. (2015) 6:295–302. doi: 10.1177/2151458515605564

77. Fulop T, Larbi A, Dupuis G, Le Page A, Frost EH, Cohen AA, et al. Immunosenescence and inflamm-aging as two sides of the same coin: friends or foes? *Front Immunol*. (2018) 8:1960. doi: 10.3389/fimmu.2017.01960

78. Si F, Liu X, Tao Y, Zhang Y, Ma F, Hsueh EC, et al. Blocking senescence and tolerogenic function of dendritic cells induced by γδ Treg cells enhances tumor-specific immunity for cancer immunotherapy. *J Immunother Cancer*. (2024) 12:e008219. doi: 10.1136/jitc-2023-008219

79. Loftus RM, Finlay DK. Immunometabolism: cellular metabolism turns immune regulator. *J Biol Chem*. (2016) 291:1–10. doi: 10.1074/jbc.R115.693903

80. O'Neill LAJ, Kishton RJ, Rathmell J. A guide to immunometabolism for immunologists. *Nat Rev Immunol*. (2016) 16:553–65. doi: 10.1038/nri.2016.70

81. Tuomisto AE, Mäkinen MJ, Väyrynen JP. Systemic inflammation in colorectal cancer: Underlying factors, effects, and prognostic significance. *World J Gastroenterol*. (2019) 25:4383–404. doi: 10.3748/wjg.v25.i31.4383

82. Triozzi PL, Stirling ER, Song Q, Westwood B, Kooshki M, Forbes ME, et al. Circulating immune bioenergetic, metabolic, and genetic signatures predict melanoma patients response to anti-PD-1 immune checkpoint blockade. *Clin Cancer Res Off J Am Assoc Cancer Res*. (2022) 28:1192–202. doi: 10.1158/1078-0432.CCR-21-3114